To the Graduate Council:

I am submitting herewith a thesis written by Constance Rebecca Eastman entitled "Preparation and Characterization of Melt Blown and Electro-Spun Polyurethane Webs." I have examined the final paper copy of this thesis for form and content and recommend that it be accepted in partial fulfillment of the requirements for the degree of Master of Science, with a major in Polymer Engineering.

Larry Wadsworth, Major Professor

We have read this thesis and recommend its acceptance:

Roberto Benson

Randy Bresee

Accepted by the Council:

Interim Dean of Graduate Studies

Thesis
2006
.E26

Preparation and Characterization of Melt Blown and Electro-Spun Polyurethane Webs

A Thesis
Presented for the
Masters of Science Degree
The University of Tennessee, Knoxville

Constance Rebecca Eastman
December 2006

DEDICATION

This thesis is dedicated to my husband and son, Patrick E.N. Eastman and Alma N. Eastman, and my dad, J.P. Higginbotham, for always supporting me in my educational goals no matter how challenging they seemed.

Acknowledgements

There are many people that I would like to thank for helping me complete my Masters of Science degree in Polymer Engineering. First, I would like to thank my advisor Dr. Larry Wadsworth for teaching me about all the many different areas of textiles and about all the machines that make the textiles of today. I would like to thank Dr. Roberto Benson for inspiring me to think and not memorize, for pushing my mind to limits I did not know I could reach, and for not allowing others to overwhelm my ideas. I would also like to thank Dr. Randy Bresee for being on my committee and for his support.

I would also like to express my gratitude for Dr. Lisa Jennings and the many others from the Health Science Center from the College of Medicine at the University of Tennessee, Memphis for this research opportunity and for the time and energy they put into testing the materials.

Special thanks to the TANDEC staff, to Chris Eash for running the melt blown equipment, to Dr. Peter Tsai for lending me his electro-spinning equipment, and to all my fellow students who have helped me along the way.

Lastly, I would like to thank my family, whose support and encouragement made all things possible for my work. Through the good times, hard times, and for their never wavering optimism I am forever grateful.

This research was sponsored by the Vascular Biology Center of Excellence at the University of Tennessee, Memphis Health Science Center from the College of Medicine as well as the Center of Excellence for Materials Processing of the University of Tennessee, Knoxville.

Abstract

Nonwoven fiber webs were formed through the processes of melt blowing and electro-spinning with the use of polyester thermoplastic polyurethane (TPU), aromatic polyether TPU, and aliphatic polycarbonate TPU. Each polyurethane was used to form fiber webs into sheets and onto stainless steel springs. Three types of fiber sheets were made: (1) melt blown, (2) electro-spun, and (3) melt blown coated with electro-spun fibers to form a composite structure. The melt blown sheets consisted of polyether TPU or aliphatic polycarbonate (PC) TPU. The electro-spun sheets were made from a 15wt% polymer solution of polyester TPU or aliphatic PC TPU. There were two composite sheets made: (1) melt blown polyether TPU covered with electro-spun polyester TPU and (2) melt blown aliphatic PC TPU with electro-spun aliphatic PC TPU. The electro-spun coatings were made from polymer solutions having concentrations ranging from 5wt% to 20wt%. The stainless steel springs were coated with the same material as the sheet samples.

Both sheets and coated springs were samples characterized in terms of their morphology and mechanical properties. The web sheets were subjected to tensile testing, porosity testing, and fiber diameter measurement. In addition, the sheets and coated springs were subjected to tests that would determine blood cell permeability and the effectiveness of the coated springs and sheets to inhibit vascular smooth muscle cell (VSMC) migration and to create new platelet activation.

Subsequent to the mechanical and morphological testing, the web sheets were evaluated for their ability to impair vascular smooth muscle cell (VSMC) migration and activate platelets growth. The melt blown polyether TPU coated with 15wt%

concentration of electro-spun polyester TPU was determined to have the best performance. This composite material was determined to be the best material due to its pore diameters (3.7 to 5.6 μm) and tensile strength (0.4 to 0.6 psi). The second best material was the composite of melt blown aliphatic PC TPU with 10wt% concentration electro-spun aliphatic PC TPU. This material had a porosity of 2 to 6.5 μm and tensile strength of 0.05 to 0.08 psi.

The composites of melt blown and electro-spun TPU are a more suitable barrier for impairing vascular smooth muscle cell (VSMC) migration. The melt blown TPU sheets contained mean pore diameters of 19 to 35 μm, which are believed to be too large to prevent the migration of VSMC. Thus, in order to reduce the pore diameters, the melt blown webs were covered by electro-spun TPU nano-fibers, which formed the composites. Although the electro-spun sheets had mean pore diameters of 0.1to 0.2 μm, the materials were too weak and fragile to be removed from the supporting paper for tensile testing and its potential strength could not be assessed prior to actual implantation.

Table of Contents

CHAPTER PAGE

I. Introduction.....1

1.1 Objective.....2

II. Background.....4

2.1 Melt Blowing.....4

2.2 Electro-spinning.....7

A. Solution Concentration.....9

B. Voltage Dependence.....9

C. Collector Distance.....11

2.3 Implantable Textiles.....11

2.4 Polyurethane.....13

2.5 Biomedical Polyurethane.....16

2.6 Materials.....17

2.7 Characterization Techniques.....17

A. Differential Scanning Calorimetery.....17

B. Porosity.....20

C. Tensile Strength.....20

D. Scanning Electron Microscopy.....21

III. Experimental Setups and Procedures.....23

3.1 Melt Blown Facility.....23

A. Extruder System.....23

B. Die Assembly.....26

C. Web Formation..... 28

D. Web Collector.....30

3.2 Electro-spinning Facility.....30

A. Electro-spinning Nozzle.....33

B. Power Source.....33

C. Web Formation.....33

D. Web Collectors..... ...34

3.3 Characterization Techniques.....34

A. Differential Scanning Calorimetry.....34

B. Porosity (PMI)..... ...36

C. Tensile Strength.....37

D. Scanning Electron Microscopy (SEM).....37

IV. Results and Discussion.....40

4.1 Materials Selection and Preparation.....40

4.2 Characterization.....41

A. Differential Scanning Calorimetry.....41

B. Porosity Testing..... .46

C. Tensile Strength..... 51

D. Scanning Electron Microscopy (SEM).....61

4.3 Fiber Coated Springs..... 69

4.4 Biological Effects..... 72

A. VSMC Proliferation in the Presence of Stimulants..... 74

B. VSMC Migration Assays..... 76

C. Platelet Activation.....78

V. Conclusion.....80

VI. Recommendations..... 82

List ofReferences..... 83

Vita..... 88

List of Tables

TABLE PAGE

Table 4. 1: ES samples concentrations and amount of materials 42

Table 4. 2: MB polyether TPU and aliphatic PC TPU porosity results..... 48

Table 4. 3: Porosity testing results for ES polyester TPU and aliphatic PC TPU. 49

Table 4. 4 Porosity testing results for composite MB polyether TPU with ES polyester TPU. 50

Table 4. 5: Porosity testing results for composite of MB and ES aliphatic PC TPU..... 52

Table 4. 6: Tensile testing results for the MB materials. 54

Table 4. 7: Tensile testing results for composite MB and ES materials. 55

Table 4. 8: Stress-strain values of MB samples. 59

Table 4. 9: Stress-strain values for composite samples. 60

Table 4.10: Fiber diameters of the MB and ES materials. 63

Table 4. 11: Fiber diameters for the composite of MB and ES materials..... 64

List of Figures

FIGURE Page

Figure 2.1: Melt-blowing manufacturing system [5]. 5

Figure 2.2: Electro-spinning manufacturing system [12]. 8

Figure 2.3: Concentration of ES PDLLA nanofibers (a) 10wt%,..... 10

Figure 2.4: The effect of target distance on SLPF fibers mixed with THF: 12

Figure 2.5: Schematic diagram of TPUs composed of diisocyanate, long chain diol, and chain extender [17]. 15

Figure 2.7: Formation of (a) poly (ether urethane), (b) poly (ester urethane), ... 19

Figure 2.8: Typical operation of a scanning electron microscope [30]. 22

Figure 3.1:Schematic of the melt blowing equipment.....24

Figure 3.2: Schematic of the extruder system..... 25

Figure 3.3: Schematic of die assembly system [19]. 27

Figure 3.4: Schematic of a die nosepiece [31, 33]..... 29

Figure 3.5: Schematic of die nosepiece and air manifold system [32]. 29

Figure 3.6: Melt-blowing collector system: (a) conveyor collector for fiber leaving the die assembly and (b) cardboard collector for nonwoven material leaving conveyor collector..... 31

Figure 3.7: Schematic of electro-spinning machine set-up..... 32

Figure 3.8: (a) Aluminum drum collector and (b) copper rod collector. 35

.Figure 3.9: (a) Melt-blown photos produced by Image Pro Plus software and 39

Figure 4.1: Plot of DSC for polyether TPU. 43

Figure 4.2: Plot of DSC for aliphatic PC TPU..... 44

Figure 4.3: Plot of DSC for polyester TPU..... 45

Figure 4.4: SEM photographs of melt-blown polyether TPU: (a) sample M1 and (b) sample M3..... 65

Figure 4.5: SEM photographs of melt-blown aliphatic PC TPU: (a) sample A1 and (b) sample A2. 66

Figure 4.6: SEM photographs of electro-spun polyether TPU and aliphatic PC TPU: (a) sample EP1, (b) sample EA1.1, and (c) EA1.2..... 67

Figure 4. 7: SEM photographs of composite of melt-blown and electro-spun fibers: (a) sample MEA1 at 5wt%, (b) sample MEA1 at 15wt%, and (c) sample MEP1 at 20wt%. 68

Figure 4.8: SEM photographs of the composite of melt-blown polyether TPU with electro-spun polyester TPU fibers: (a) MEP1 at 10wt%, (b) MEP1 at 15wt%, ... 70

Figure 4.9: SEM photographs of the composite of melt-blown aliphatic PC TPU and electro-spun aliphatic PC TPU: (a) MEA2 at 10wt% and (b) MEA2 at 20wt%. 71

Figure 4.10: 4mm stainless steel springs: (a) electro-spinning process and (b) top: bare metal spring, middle: electro-spun fiber coated on spring, bottom: melt-blown fibers coated on electro-spun fiber..... 73

Figure 4.11: Vascular smooth muscle cell proliferation of springs with stimulant results. 75

Figure 4.12: Vascular smooth muscle cell migration assay results. 77

I. Introduction

Over the years there has been a vast amount of improvements made within the biomedical community. From sutures to pacemakers, the importance on improving and prolonging life has become an economical rainstorm, with new ideas and devices being made every day. The biomedical world has grown so fast and far that it has embraced other areas of technology. Some of those areas include melt blowing and electro-spinning techniques of the textile industry. It is the merging of biomedical technology with textile processing technology that has warranted an academic study.

The melt blowing process is usually known for the creation of nonwoven fabrics that are used in air filtration, hospital gowns and masks, and diapers. The process is a single step process to convert polymer granules or pellets into the fiber webs. In most cases the technology is used to make fibers for exterior wear, but this research is investigating melt blown (MB) materials that may be used within the body. The most common polymer used for MB is polypropylene (PP), but polyethyleneterephthalate (PET) and thermoplastic polyurethane (TPU) are being studied for use in the body.

The electro-spinning (ES) process utilizes the techniques of electro spraying and the commercial spinning of fibers to form nano-fibers. The process usually requires dissolving of the polymer in a solvent, which is then spun [1]. The polymers used in the process include nylon 6, polyurethanes, biodegradable and bioabsorbable polymers from polyacetic acid and polyglycolic acid, among others.

Historically, most of the research done using biomedical devices with textile technology has dealt with vascular graphs. The vascular system has been studied extensively since the early 1900s due to the damaging of veins. The most common grafts

used today are biological and synthetic grafts. Biological grafts, such as autografts, are veins taken from other parts of the vascular system and used to repair the damaged vein. Synthetic grafts used today are formed from PTFE and are used more than biological grafts due to availability of autografts. Even though autografts and PTFE grafts have had good success after implantation, each graft still allows thrombosis and infection to occur. Through the use of melt blown and electro-spun polymers, nonwoven webs were created in order to decrease thrombosis and infection [2].

The research presented here determines whether MB, ES, or a composite of MB and ES polyurethanes will create a material that will impair vascular smooth muscle cell (VSMC) migration and activate platelets. The research will also analyze the test results and suggest improvements to the materials, such as a drug delivery system, that could be in a future study.

1.1 Objective

The purpose of this research was divided into the following three tasks:

Task 1: Material Preparation

A. Evaluate the candidate polymers with respect to hemocompatibility and biocompatibility.
B. Develop electrostatic fiber spinning (ES) and fiber collection techniques to adhere the nano-fibers to flat sheets and to springs.
C. Develop melt blowing (MB) and fiber collection techniques to adhere the micro-fibers to flat sheets and to the outside of springs.
D. Develop micro-fiber and nano-fiber layered structures using ES and MB techniques to make the optimal porosity and mechanical properties.

Task 2: Material Characterization

A. Evaluate candidate polymers with respect to mechanical compatibility: tensile properties and porosity (PMI).
B. Evaluate candidate polymers with respect to processibility: Differential Scanning Calorimetery (DSC).

C. Characterize the candidate polymers structure: Using Scanning Electron Microscope (SEM) to photograph the web.
D. Form polymer solutions with respect to solvents (DMF and THF) and to evaluate the polymer solutions after fiber formation.

Task 3: Determine biological effects

A. Determine VSMC proliferation of the fiber covered springs.
B. Determine the effectiveness of the sheets to inhibit VSMC migration and to activate platelets.

II. Background

2.1 Melt Blowing

Melt blowing (MB) is defined as the "process in which usually a thermoplastic, fiber forming polymer is extruded through a linear die containing several hundred small orifices. Converging streams of hot air (exiting from top and bottom sides of the nosepiece) rapidly attenuate the extruded polymer streams to form extremely fine diameter fibers (1-5 um). The attenuated fibers subsequently get blown by high velocity air onto a collector screen-thus forming a fine fibered self-bonded nonwoven melt blown web" [3]. There are some cases when MB is a batt of loose fibers used for ultrafine filters for face masks, personal hygiene products, oil spill absorbents, and air conditioning. MB batt is also known to be laminated to another nonwoven material, such as spun laid , and used in breathable protective clothing in hospitals, industry, and agriculture [4].

The MB process, however, is more complicated that it seems. Figure 2.1 shows an example of a normal MB machine. The machine is made up of many different parts, which are: (a) a hopper, (b) an extruder, (c) extrusion head dies, and (d) a collector that consists of a drum, continuous band, or an immovable part. The polymer granules are placed into part (a) of the machine, which are then funneled into the extruder. By controlling the rotational speed and the gradient temperature of the extruder, the polymer is processed. After melting, the polymer is forced through the extrusion head dies by use of an air flow pipe and projected onto a collector as fibers. The fibrous spray is regulated by the air flow pressure, temperature, distance between the die tip nozzle and collector, and velocity of the collector. Changing the pressure, temperature, or collector distance

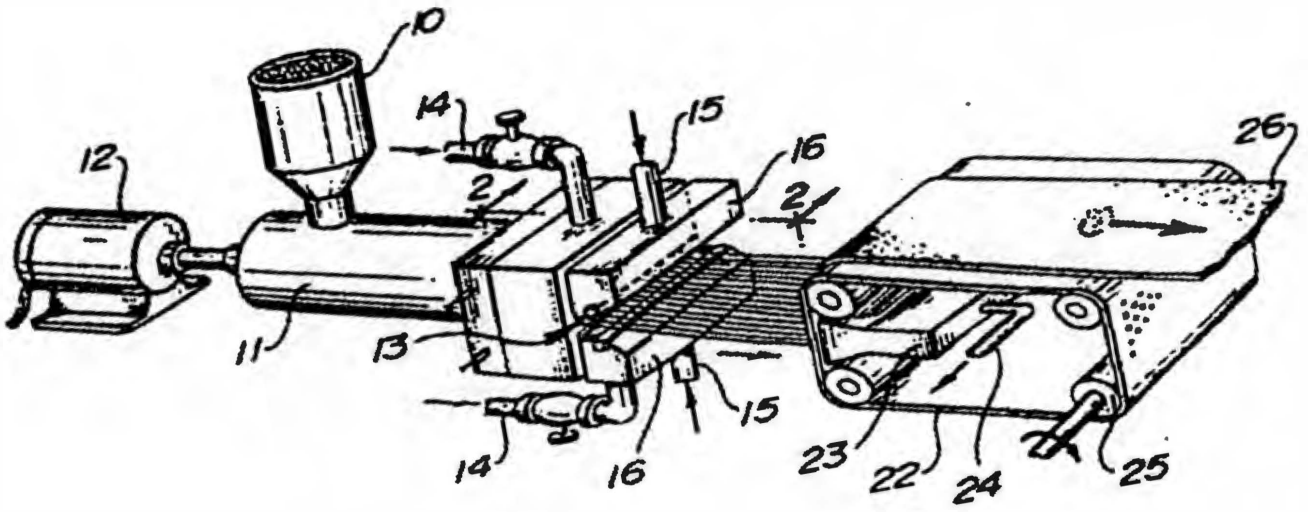

Figure 2.1: Melt-blowing manufacturing system [5].

will change the thickness of the webs and diameter of the fibers. Each parameter can be adjusted until the desired fibers are formed, which is why melt blowing attracts many different areas of manufacturing and designing.

The melt blowing process has advanced since the early 1950's, when the use of this fiber formation technology came about. As time passed, the Cold War furthered the need for MB fibers when there came a need for a micro-fibrous polymer absorbent that could capture radioactive particles in upper atmospheric layers. Later in 1965 Exxon began to use the technology to research applications for polypropylene, and then between the 1970's and 1990's melt blowing emerged as an important commercial process with several patents being issued [6].

Pinchuk et al. [6] stated that as the years have progressed MB has become a cost effective way to produce nonwoven fabrics for a wide range of applications. It is also known for being able to vary the materials structure and properties. Some of the products are used in households, industry, construction, medicine, and the environment. The household products include towels, hygienic napkins, disposable clothes, and diapers. Industrial MB products are used for filtration, insulation, and absorbent materials. In construction there are floor and lining materials, such as mats used for heat and soundproofing coatings [7]. In the environment area there are materials that hinder soil erosion. The materials that hinder soil erosion are made by sandwiching a layer of MB material between two layers of spun-bond material, which form a layer of weed protection [8]. As for medicine, there are surgical drapes and gowns, face masks, bandages and splints, burn dressing, and even a vessel endoprostheses [9].

2.2 Electro-spinning

Electro-spinning (ES) has been around since 1934 when Antonin Formhals patented the process. The ES process creates fibers with diameters in the range of nanometers to a few μm, and the fibers are known to have diameters that are 5 to 10 times smaller than that of the smallest melt blown fiber that is available today [10]. Figure 2.2 shows a schematic of an electro-spinning machine. It consists of a syringe, needle, polymer solution, a high voltage supply, a metering pump, and a collector that can be stationary or rotating. The polymer solution is placed inside the syringe that is tipped off with a needle. The syringe is then placed into a metering pump that uses force to push the solution out of the tip of the needle. The voltage supply is connected to the needle and also to a ground supply and the voltage used can be generated up to 30kV. The voltage is applied to the tip of the needle causing the polymer to be stretched into a Taylor cone. As the polymer is sprayed out of the syringe into a Taylor cone it undergoes a whipping process that allows the solvents within the solution to evaporate forming a polymer fiber that is deposited onto a collector.

Most ES research has been done on the types of solvent systems used for nano-fiber spinning and little research for the processing-property relationships. The processing parameters studied included the solution concentrations, target distance from the needle tip, feed rate of the fluid to the needle tip, and the spinning voltage. The solution concentration, spinning voltage, and the distance of the collector from the syringe are the parameters that determine the amount of fibers produced [11].

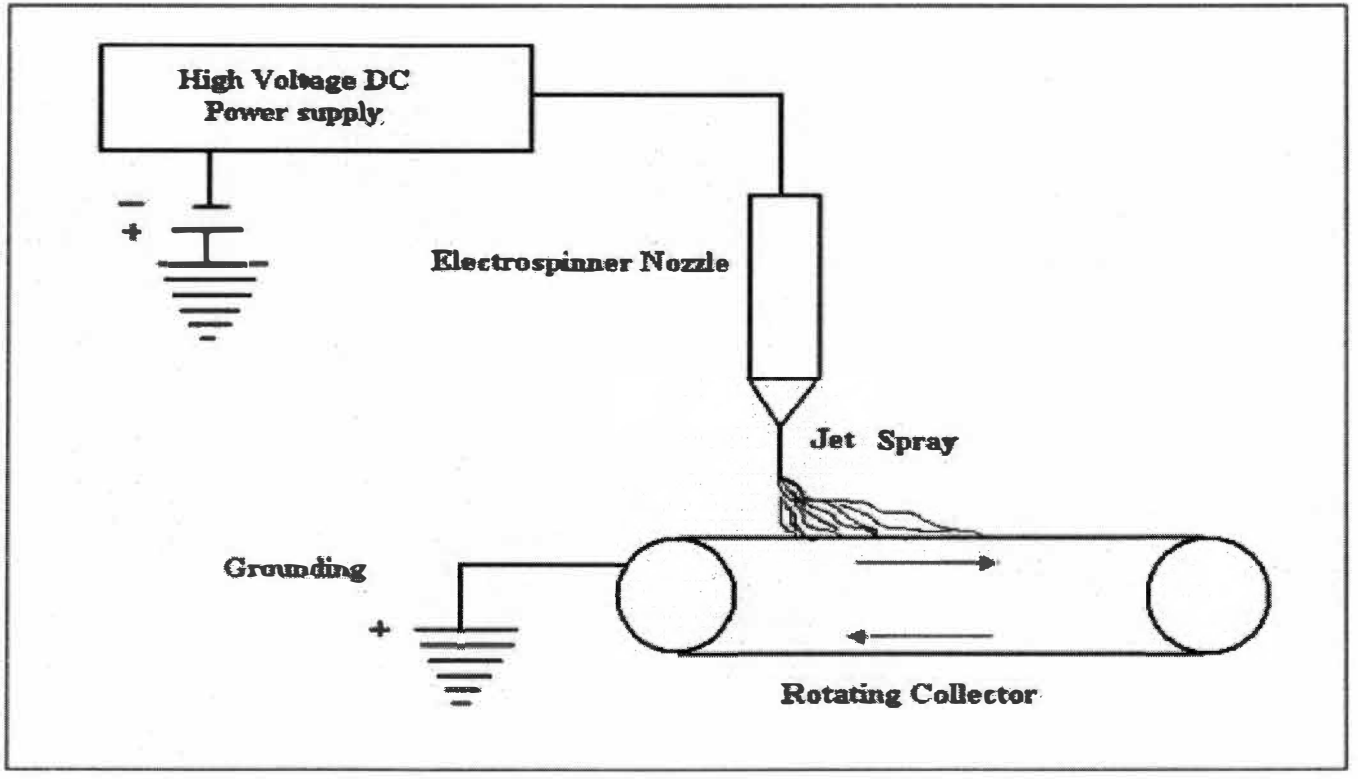

Figure 2.2: Electro-spinning manufacturing system [12].

A. Solution Concentration

The ES fiber diameters are dependent on the solution's viscosity, which also influences the droplet shape and jet trajectory [10]. Deitzel studied the fiber formation of poly(ethylene oxide) of solution concentrations of 4-10%. It was observed that when the concentrations were below 4% that a mixture of fibers and droplets were formed. When the concentrations were above 10% the high viscosity of the solution made it hard to force it through the syringe. It was also observed that lower concentrations produced irregular fibers with varying diameters and higher concentrations produced more uniform fibers [11]. The higher concentrations contained more uniform fibers because they have enough entanglements to prevent droplets from occurring. Deitzel also observed that the electro-spun fiber diameters increased when the concentrations increased by the power law relationship [11]. Figure 2.3 shows the fiber formation with respect to solution concentrations of PDLLA in DMF.

B. Voltage Dependence

In order for fibers to be produced through the ES process, the applied voltage must be high enough to overcome the surface tension of the solution. The applied voltage is measured with a high velocity micro-amp meter and used to control the amount of polymer that reaches the collector. At a low voltage, a droplet of solution remains at the end of the needle because the voltage potential does not exceed the surface tension. The fiber jet originates at the bottom of the droplet. The fibers produced at low voltages are usually cylindrical with some bead defects. The bead defects are undesirable "by products" that are produced when there is instability of the jet of polymer solution [13]. As the voltage increases the fibers are still cylindrical but they may contain more bead

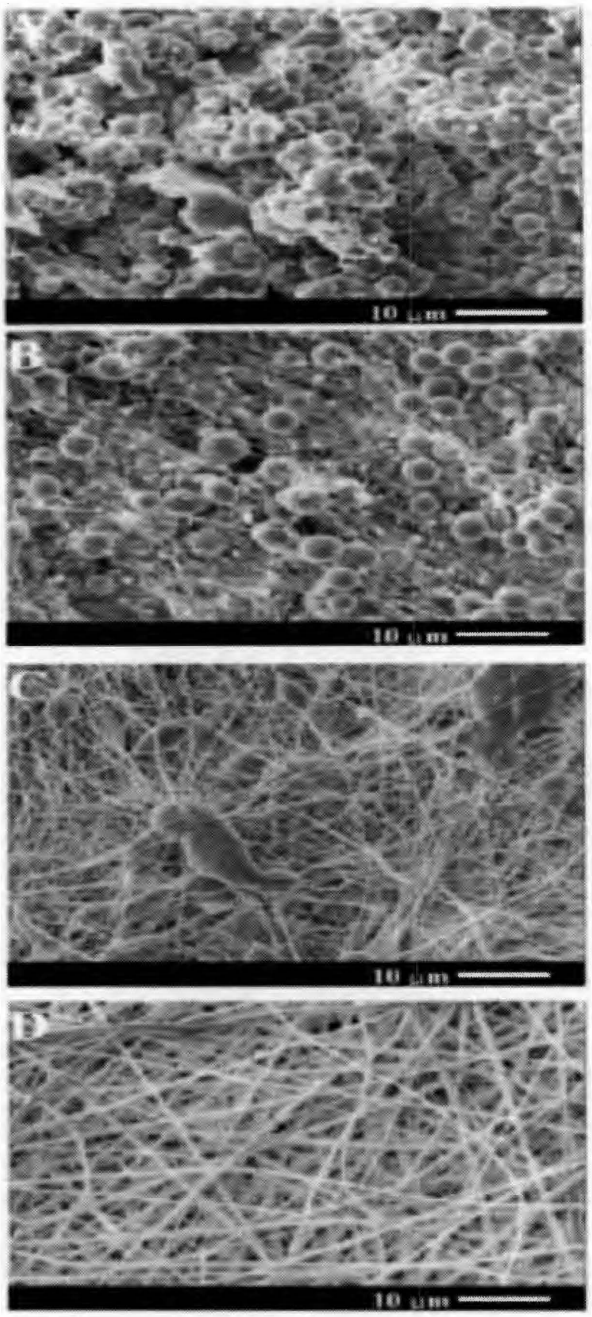

Figure 2.3: Concentration of ES PDLLA nanofibers (a) 10wt%,

(b) 25wt%, (c) 30wt%, and (d) 35wt% [14].

defects due to the jet originating from surface of the solution at the needle tip. In order to control the amount of bead defects, the applied voltage must be optimized with respect to the solution.

C. Collector Distance

The distance of the collector from the needle tip will determine the formation of the fiber structure. For short collection distances, the fibers will have a more membrane like structure because not all of the solvents will be evaporated. For long collection distances, the fibers have a more uniform structure due to the solvents evaporating completely. The collector distance will also affect the fiber sizes. Figure 2.4 illustrates the difference between the distances of 0.5cm and 2cm for a Silk like polymer with Fibronectin functionality (SLPF) that were spun from THF [15].

2.3 Implantable Textiles

Implantable textiles are used in effecting repair to the body as vascular graphs, artificial ligaments, and more. There are five key factors that determine how the body will react to the textile implant. The first factor is that the material must be biocompatible, which is the prime factor for all biomedical devices. The second factor is porosity because it determines the rate that human tissue will grow and encapsulate the implant. The third factor is that the textile fibers should be small and circular because they can be better encapsulated by human tissue than larger irregular cross-sectioned fibers, if encapsulation is desired. The fourth factor is that toxic substances should not be released by the textile material. They must also be free from surface contaminants such as lubricants and sizing agents. The last factor is the materials biodegradability that will influence the success of the implantation [4]. Since the materials used in this research are

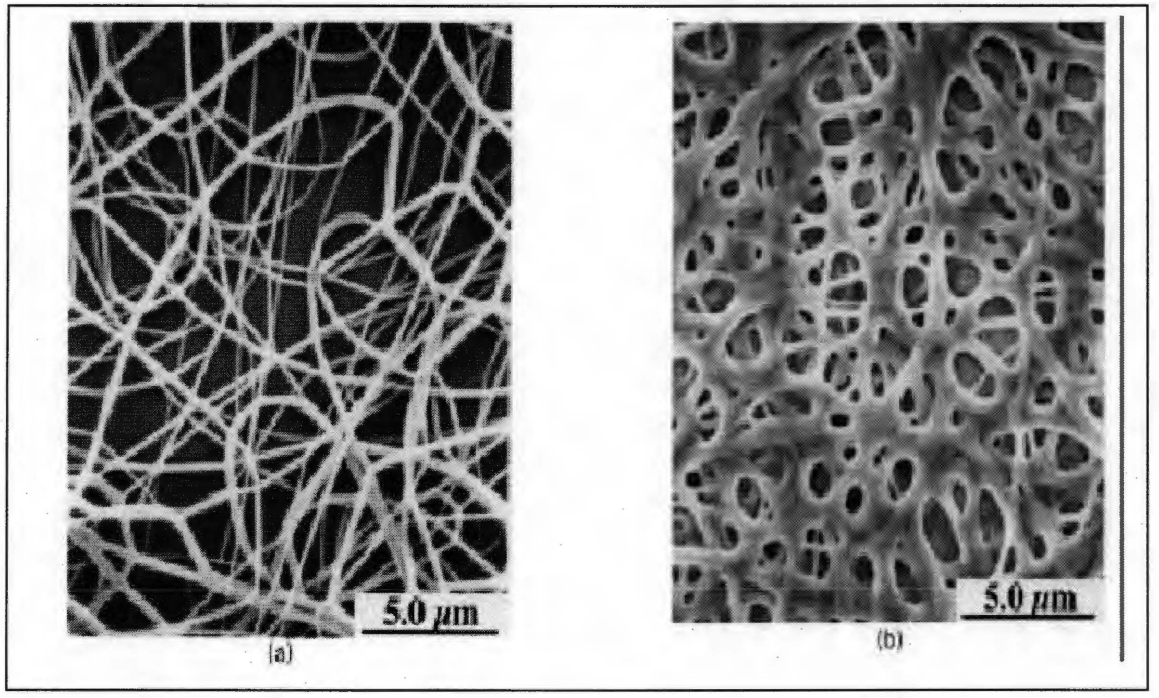

Figure 2.4: The effect of target distance on SLPF fibers mixed with THF: (a) 2cm and (b) 5cm [11].

textiles that are made through melt blowing and electro-spinning, they must meet all the key factors. Melt blowing and electro-spinning are currently being used for artificial cartilage and vascular graphs [4].

2.4 Polyurethane

Polyurethanes are organic polymers that have been around since 1937 when Otto Bayer, along with his coworkers, discovered and patented the chemistry of polyurethanes. It was not until 1940, however, that polyurethanes began to be used. In 1940, polyurethanes were used as rigid foam in aircrafts. As the years progressed, the uses of polyurethanes expanded to produce adhesives, insulation, synthetic rubbers, foam cushions, shoe soles, automobile bumpers, imitation wood, foams, tires, and orthopedic and medical applications [16].

Even though polyurethanes are used in many different applications, it is the underlying chemistry that is the most intriguing. Polyurethanes are made up of a soft segment and a hard segment. The soft segments are usually a low molecular weight polyether or polyester. It is the polyether that contains a high molecular weight and a wide range of viscosities, which are used to form polyurethanes that are flexible foams or thermoset elastomers. The hydroxyl terminated soft segments are reacted with the diisocyanate or isocyanate in the presence of additives and a catalyst, leading to the formation of the polyurethane. Polyurethanes may be rigid, flexible, adhesive, thermoset, and thermoplastic materials.

Thermoplastic polyurethanes are the polyurethanes used in this research. TPU's are known as polyurethane elastomers used in footwear, machinery housings, and even electronic media devices. It is their mechanical properties of elasticity, toughness,

strength, and low temperature flexibility that allow them to be used in various engineering applications. Thermoplastic PU's soften when heated and harden when cooled due to their elastomeric properties. They consist of long chains of molecules that contain smaller, repeating units, and form the arrangements of soft and hard segments [17]. The soft segments formed are from flexible oligomers with low glass transition temperatures, which causes the TPU's to be flexible at room temperature. The hard segments act like thermally reversible physical cross-linking mechanisms that are between molecular domains. A typical composition of a TPU can be seen in figure 2.5.

In this research, there is an polyester based and an polyether based TPU. For each TPU, the properties are based upon their soft and hard segments. Szycher studied the hard segments of TPUs and provided information about chain extenders and diisocyanate [18]. This study concluded that diphenylmethane-4,4'-diisocyanate (MDI) was the most important diisocyanate [18]. Xiao and Frisch stated that within the diisocyanate the hydrogen bonding between the adjacent polymer chains forms the three dimensional "virtually cross-linked" molecular domain structures [19]. The inter-chain attractive forces between the rigid segments are greater than those in the soft segment because of the high concentration of polar groups and formation of extensive hydrogen bonding [20].

Rigid polyurethanes are usually foams that are used as insulation for water heaters, buildings, and flotation devices. Flexible foam polyurethanes are used for cushioning in carpets, furniture, and packing. The adhesive foams are seen in construction, transportation, and many other areas that require a material with high strength, moisture resistant, but yet durable. Thermoset polyurethanes are widely used

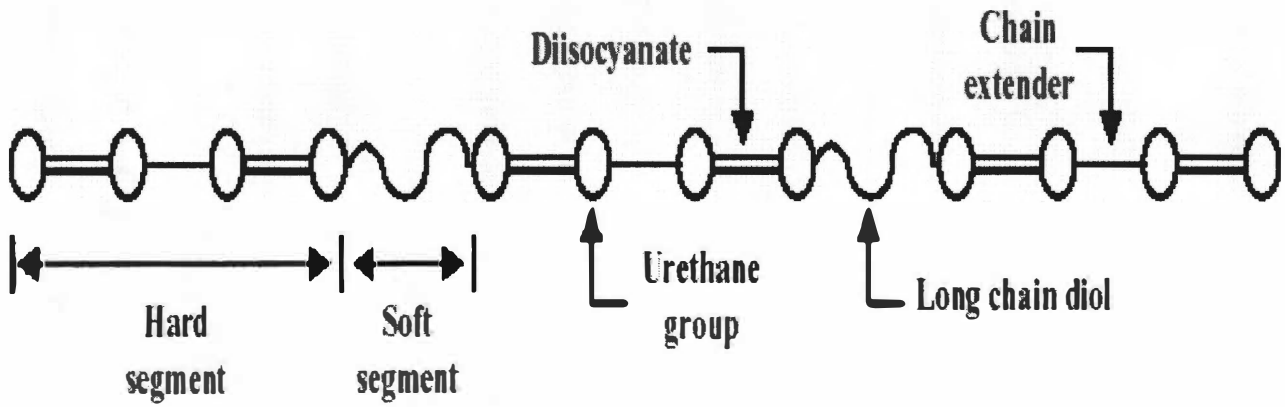

Figure 2.5: Schematic diagram of TPUs composed of diisocyanate, long chain diol, and chain extender [17].

materials and they cannot be melted and reshaped. Thermoset PUs are made by combining urethane with isocyanate linkages. "At least one portion of the catalyst is applied onto the surface of the reinforcing fibers" [15] or uncured resin, where the conditions are such that the catalyst is not dispersed into the bulk of the isocyanate that contains the resin until it is cured [15, 21].

2.5 Biomedical Polyurethanes

Polyurethanes are one type of polymer that is used for blood contacting devices [8] and because they are used within the human body these polyurethanes have more regulations and guidelines placed upon them than other forms of polyurethanes. In order for polyurethanes to be used in the human body, it is necessary that they be bio and hemo compatible. Materials are biocompatible if the materials or their degradation products do not elicit adverse response within the body. Materials are blood compatible if the properties of the materials allow the device to function while in contact with blood without causing adverse reactions such as clotting, leaching of toxic materials, killing blood cells, or causing any molecular change to the body.

Biocompatibility and blood compatibility are not the only important aspects to determining biomedical polyurethanes. In order for polyurethanes to be considered suitable for biomedical applications, they need to be non-toxic. In other words, the device must not cause death, alterations in cellular membrane permeability, enzymatic inhibition, or any other defects to the cellular level. The device must not directly or indirectly kill cells, or cause leaching within the body. It must also not cause sensitizations or irritations, and must be hemocompatible.

There are many types of biomedical polyurethanes, such as polyester, polyether,

polycaprolactone, polybutadiene, and castor oil based. Polyether-based polyurethanes are more widely used since they are not as easily hydrolyzed in the body as polyester based PUs. PUs that are composed of 100% aliphatic PC components are said to be more biocompatible for long term use in the human body [22]. They have the ability to be stable in the physiological environment. Once in the human body, polyester based polyurethanes can undergo hydrolysis, while castor oil based has poor tear resistance. As for polycaprolactone-based polyurethanes they are mainly used as medical adhesives and polybutadiene-based polyurethanes have limited medical use even though they have undergone several evaluations. In the end, all the biomedical polyurethanes used in the human body must undergo intense evaluations until they are deemed acceptable for biomedical use [23, 24].

2.6 Materials

The three materials chosen in this research were a polyester-based TPU, an aromatic polyether-based TPU, and an aliphatic PC polycarbonate-based TPU. The synthesis of polyurethane is illustrated in figure 2.6. The polyester and polyether TPU was synthesized using methylene diisocyanate (MDI) with a polytetramethylene glycol. The polycarbonate TPU was synthesized using hydrogenated methylene diisocyanate (HMDI) with a polycarbonate diol. A polyester TPU, polyether TPU, and polycarbonate TPU are illustrated in figure 2.7 [25].

2.7 Characterization Techniques

A. Differential Scanning Calorimetry

Differential scanning calorimetry (DSC) uses the differences in the heat flow of a sample to measure melting temperatures, glass transition temperatures, and crystallinity.

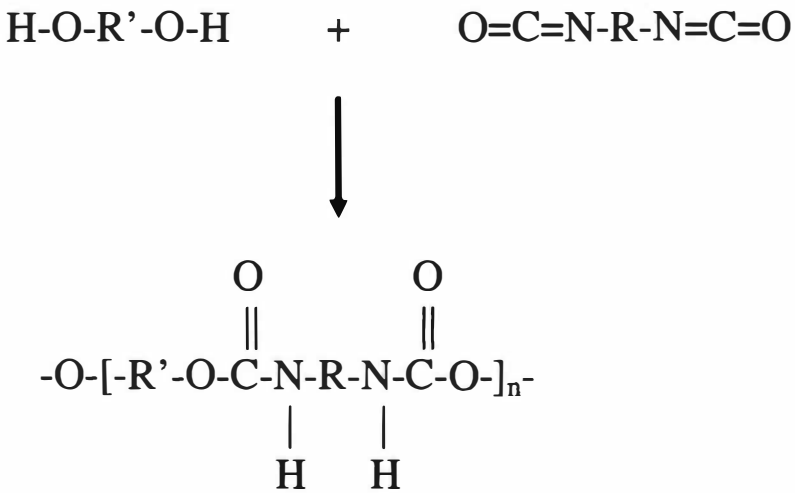

Figure 2.6: Formation of polyurethane [26].

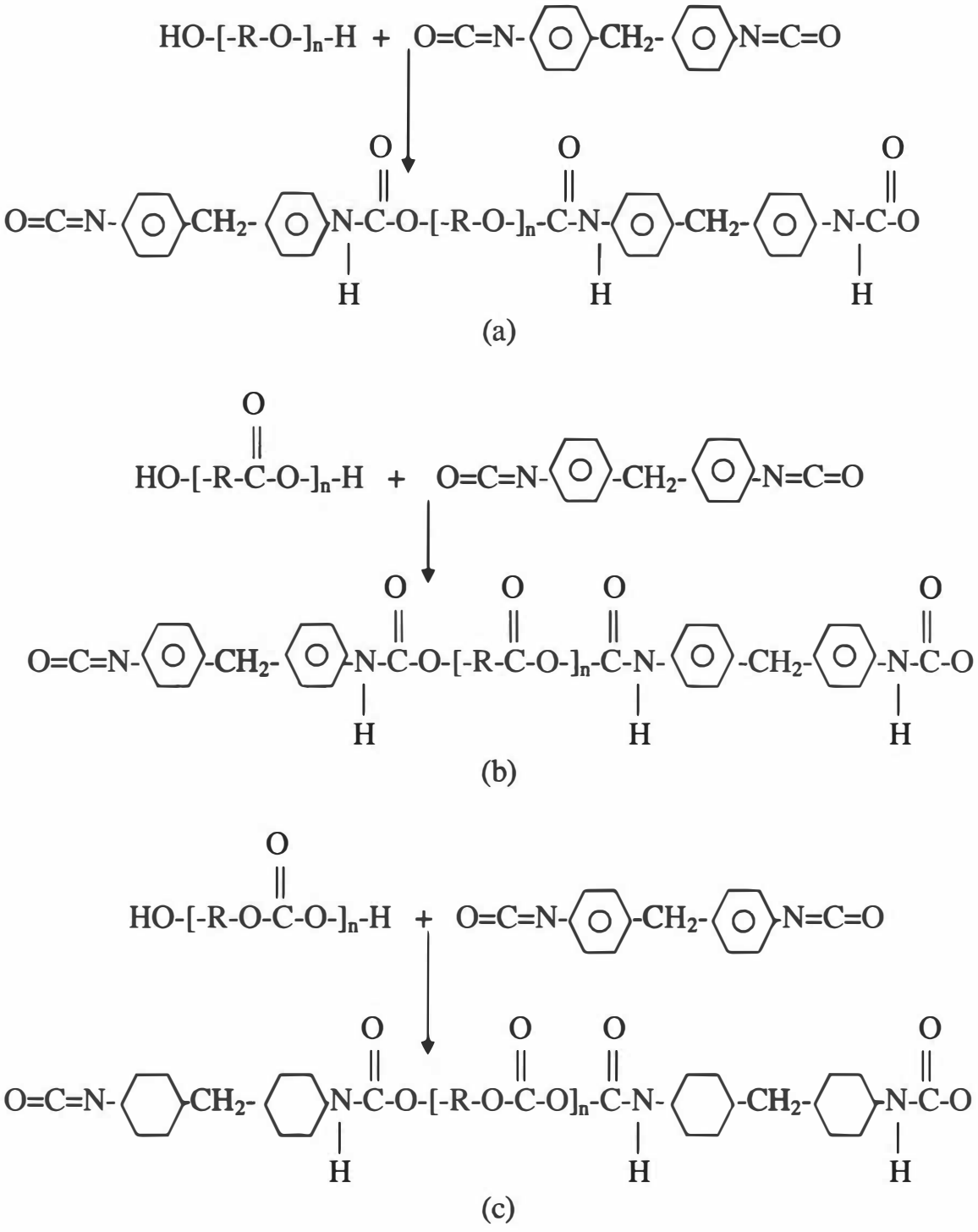

Figure 2.7: Formation of (a) poly (ether urethane), (b) poly (ester urethane), and (c) poly (carbonate urethane) [27].

The DSC process consists of a sample pan and a standard pan, which are heated simultaneously. Both pans are heated at a constant rate, which allows a reference line to be used to monitor any transitions. As the sample is heated, an exothermic or endothermic transition will occur causing the heat flow to increase or decrease depending on the type of transition. After heating is completed, a plot of differential power heat flow versus temperature is produced. From the plot, the melting temperature, glass transition temperature, and crystallinity can be found.

B. Porosity

A capillary flow porometer (PMI) uses airflow to measure pore diameters and pore pressures. A pore is a hole that resides with the material and the pressure is how much airflow it takes to pass through the pore. The PMI process consists of cylindrical disk with a 0.8cm circular whole at the center. A $5in^2$ sample was cut from each set of material, wetted, and placed into an airtight chamber. As air is released at a constant rate between 0 and 25psi through the chamber, the maximum and minimum pore diameters and pressures are found. The pore diameter and pressure data is displayed in an excel file and analyzed in order to determine the average pore diameters and pressures for each sample.

C. Tensile Strength

The Economy SSTM Series and the Multi-Station Model MS Series tensile testers used 10lb weights to measure the amount of force and elongation each sample can undergo before breaking occurs. The tensile testers use a computer program to analyze the data from a formation plot and form a list of forces and elongations for each sample

tested. The forces and elongation data is then used to calculate stress and strain for each sample in order to determine the strengths of materials.

D. Scanning Electron Microscopy

A scanning electron microscope (SEM) is an instrument that uses optical microscopes to obtain images of solid objects. It uses an electron gun, vacuum column, a lens system, electron collector, an electron beam, and visual and recording cathode ray tubes (CRT) to examine and analyze the microstructures of the specimens. Figure 2.8 shows a typical SEM's operation. An advantage of SEM is that it provides more information about the specimen due to its large depth of field, which gives a three dimensional appearance of the specimen [11, 28].

Through the use of the vacuum column an electron beam enters the sample chamber and strikes the specimen at a single location. The beam consists of high-energy electrons that are emitted from the electron gun down the column through a series of magnetic lenses. The magnetic lenses consist of a condensing lens and an objective lens placed within the column in order to focus the electrons onto a very fine spot. The focusing of the electron beam was also controlled by the scanning coils, which move across the sample in an X-Y pattern to allow the electron beam to hit different spots on the sample. Once the electron beam hits a spot on the sample, it causes secondary electrons to be removed from the samples surface. A detector that sends the signals to the amplifier then counts the secondary electrons and transfers that information to the CRT [29]. Figure 2.8 shows the correspondence between the scanned specimen and the transfer of data to the CRT [30].

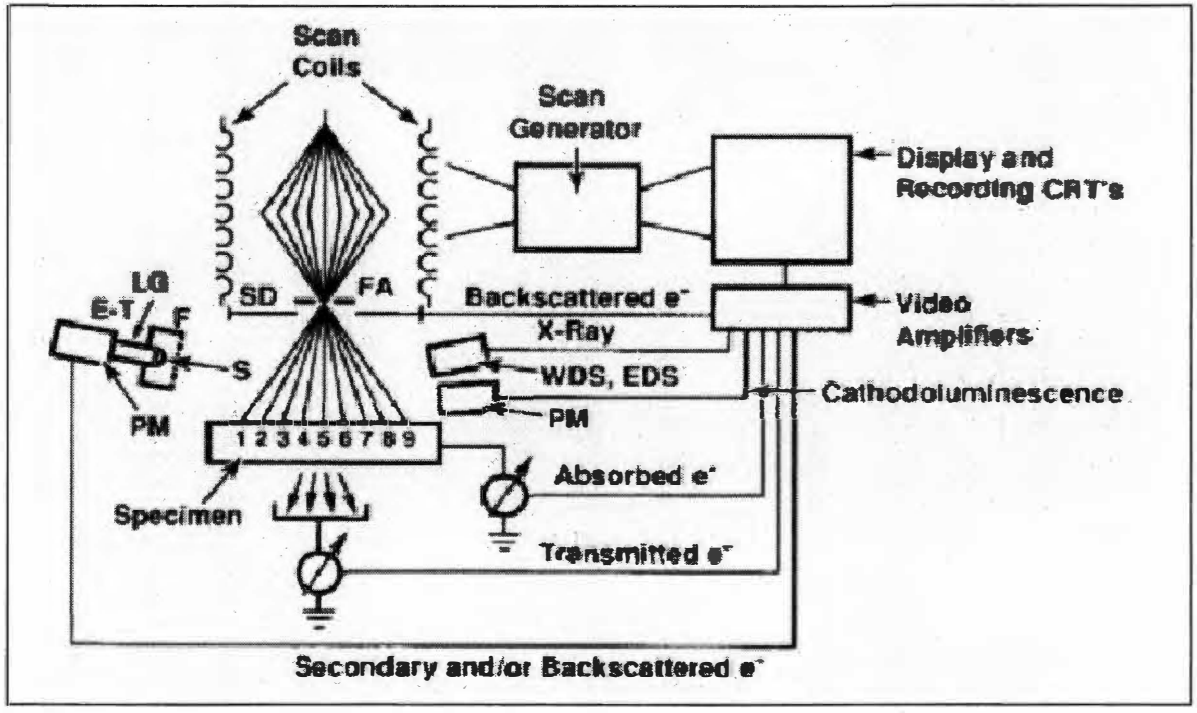

Figure 2.8: Typical operation of a scanning electron microscope [30].

III. Experimental Setups and Procedures

Chapter III describes the experimental machines that were used to form melt blown (MB) and electro-spun (ES) webs for this study. This chapter also describes the processes for analyzing the fiber diameters of the webs. The discussion of this chapter is divided into three sections. The first section discusses the melt blowing machine, which includes the formation and collection elements. The second section discusses the electro-spinning apparatus, along with the formation and collection of electro-spun fabrics. The third section discusses the analysis of the nonwoven webs thru the use of PMI, tensile, SEM, and Image Pro Plus.

3.1 Melt Blowing Facility

The melt-blowing machine used in this research is located on the ground floor of the Textiles and Nonwovens Development Center (TANDEC) building at the University of Tennessee, Knoxville. The machine is made up of the following parts: (1) extruder, (2) die assembly, (3) web formation, and (4) web collector. Figure 3.1 shows a schematic the melt-blowing machine.

A. Extruder System

The extruder constitutes the initial component of the melt-blowing process. Figure 3.2 shows the schematic of the extruder system, which consists of a rotating screw and a heated barrel. The extruder causes the polymer pellets or granules to melt, which turns the polymer into a fluid. "The melting of the polymer is due in part to the heat and the friction of the viscous flow and the mechanical action between the screw and the walls of the barrel" [31]. Within the extruder are three heating zones. The first zone is the feed zone. This zone is where the polymer pellets or granules are preheated before entering

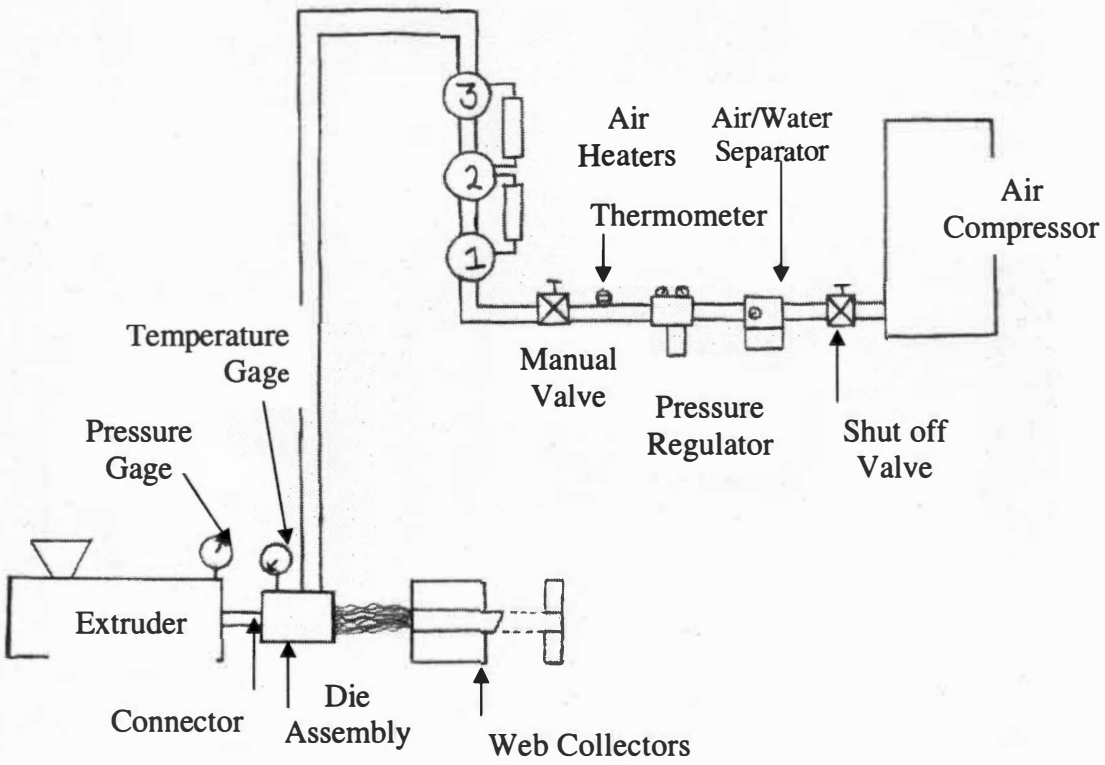

Figure 3.1:Schematic of the melt blowing equipment.

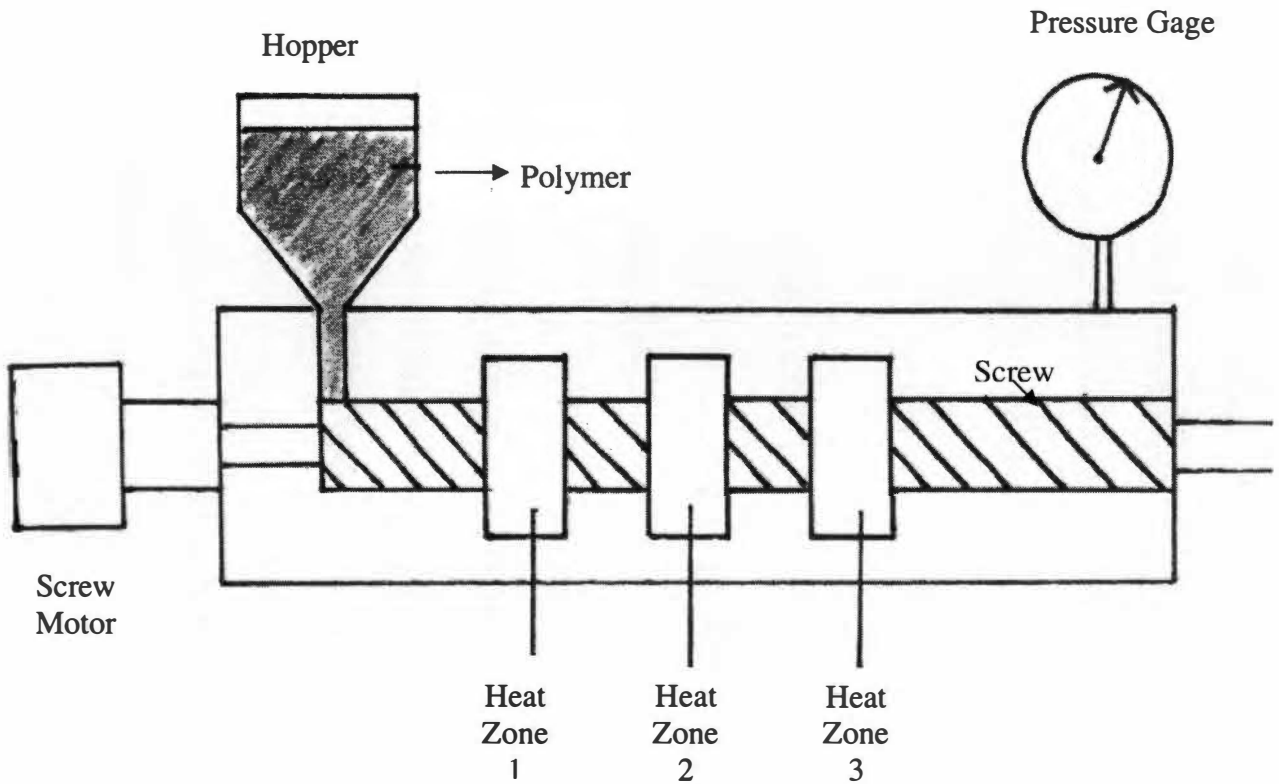

Figure 3.2: Schematic of the extruder system.

the second zone. The second zone is the transition zone. In the transition zone the preheated polymer is compressed and homogenized in the zones decreasing depth channel. Once the polymer is compressed and homogenized, then it enters the third zone called metering zone. In the metering zone the polymer is pushed in the forward direction by using the zones ability to generate the maximum pressure needed to pump the melted polymer. In this zone any impurities are filtered out by a breaker plate that is within the metering zone. As for the three heaters they are distributed within the zones so that there is one heater in each zone [31].

B. Die Assembly

Once the melted polymer leaves the extruder through a filtering screen it enters the die assembly, which is considered the most important part of the melt blown process. The die assembly consists of a polymer feed distribution, die nosepiece, and an air manifold. Figure 3.3 shows the setup for the die assembly.

As the melt polymer is pushed through the extruder it enters the feed distribution component of the die assembly. This component is designed so that the polymer is not very dependent on the shear properties of the polymer. The feed distribution is considered very important in melt blowing because molten polymer does not usually have mechanical means to compensate for any changes or variations that may occur in the flow across the die width. Also, the feed distribution is able to operate at temperatures that allow the polymer to undergo thermal breakdown quickly. In all, there are two forms of feed distribution: T-type and coat hanger. In most cases coat hanger is used because of its ability to provide more even flow and residence time across the width of the die. The die nosepiece is another part of the die assembly and this component lies at the end of the

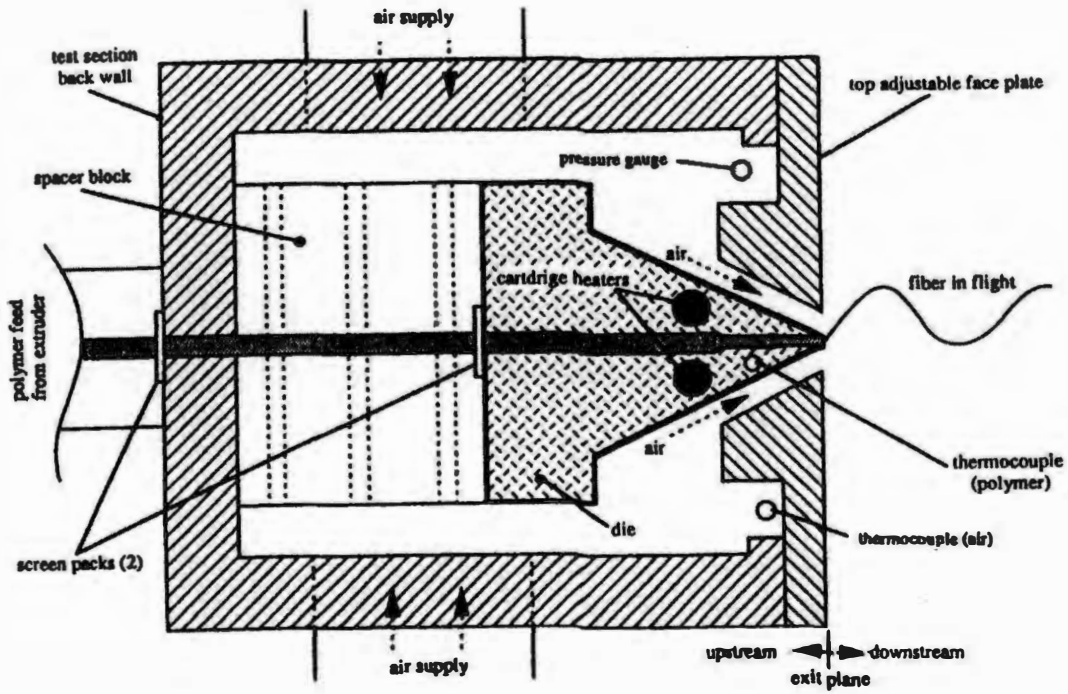

Figure 3.3: Schematic of die assembly system [19].

feed distribution section. The die nosepiece is made up of metal that is tapered, hollow, wide, and possesses very tight tolerances. This component also includes several hundred orifices that lay across the width of the die tip. The die nosepiece used in the research was a drilled hole type, which contains orifices that were drilled into a single block of metal. The die nosepiece consisted of a 60° angle nose tip with 25 spinneret holes per linear inch with 15 mils orifice diameters, a 30 mil die tip set back form the outer edge of the air knife, and a 30 mils air gap between the inside plane of each air knife and die nose tip. Figure 3.4 shows the die nosepiece set up.

The last component of the die assembly is that of the air manifold. The air manifold provides high velocity hot air into the die assembly's nosepiece. The high velocity air comes from an air compressor that runs the air thru an electrical furnace heat exchanger. The air manifold, itself, is made up of three vertically aligned air heaters as shown in figure 3.5. The air heaters were run at power settings of 125 KW for heater one, 48 KW for heater two, and 12 KW for heater three. As seen in figure 3.1, the heaters run vertically aligned so that the air flows from heater one into heater two then into heater three. Once the air passes thru heater three it is forced through a pipe that is connected to the die nosepiece. Once in the nosepiece, the high velocity hot air is funneled through the air gaps causing the molten polymer to be released from the melt blowing machine and onto a collector [32].

C. Web Formation

The fourth part of melt blowing is the formation of the fiber webs. Once the high velocity hot air is forced into the die assembly, the molten polymer streams out to form micro-fibers. After the molten polymer leaves the die nosepiece a stream of cool air is

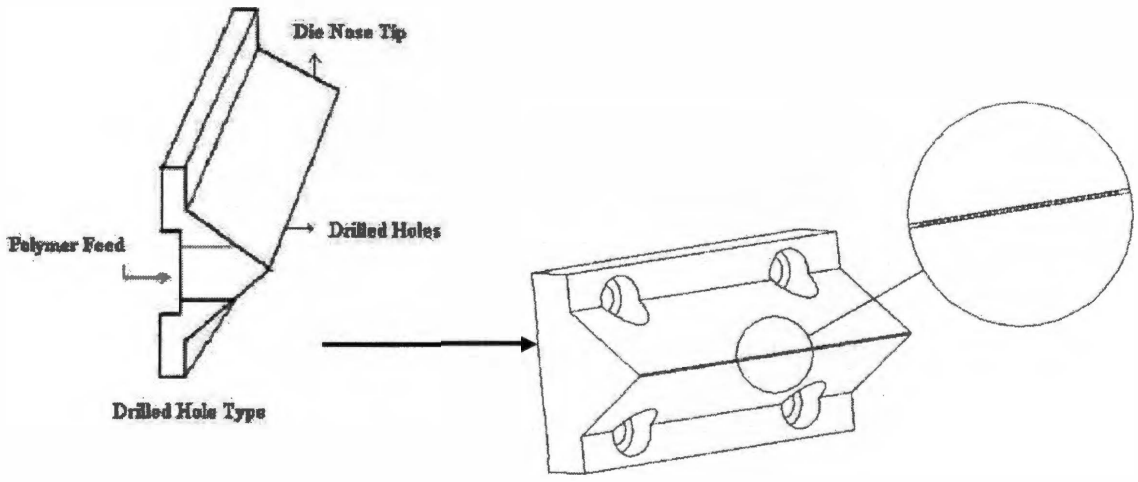

Figure 3.4: Schematic of a die nosepiece [31, 33].

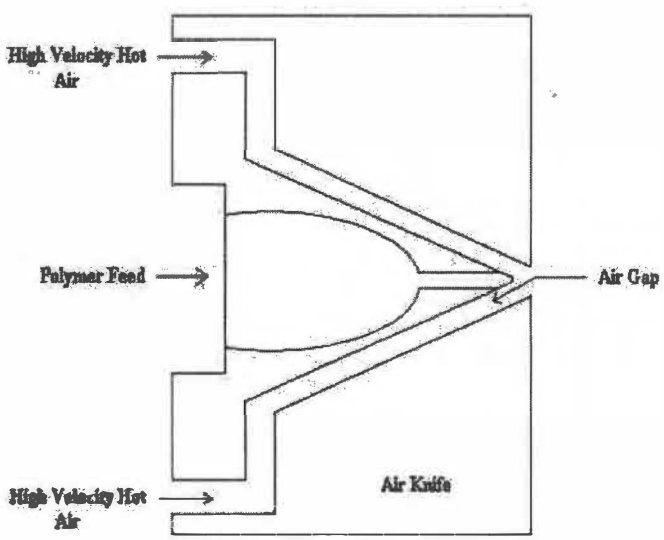

Figure 3.5: Schematic of die nosepiece and air manifold system [32].

drawn in so that the fibers will solidify before being laid unto the collector. Once the fibers are cooled they are laid onto the collector forming a nonwoven web that is self-bonded. The formation of the webs are due to the turbulence that is formed by the air stream and by the movement of the collector [32].

D. Web Collector

The web collector is the final part of the melt blowing process. The purpose of the web collector is to collect the fibers after they have solidified. For the present research, the collector consisted of two parts. The first part was a conveyor belt that ran in a circular motion. The conveyor belt was the device that originally collected the newly formed fiber webs. Once the webs were on the conveyor belt, they were sent to the second part of the collector system. The second part was a cardboard core that was attached to a motor that rotated the core as the fibers were being attached. The webs were wound onto the cardboard core from the conveyor belt and later the cardboard core was removed along with the webs so that the webs could undergo further processing and testing. Figure 3.6 shows the collector system.

3.2 Electro-spinning Facility

The electro-spinning machine used in this research is located on the second floor of the TANDEC building at the University of Tennessee, Knoxville. The machine is made up of the following parts: (1) electro-spinner nozzle, (2) power source, (3) web formation, and (4) web collector. Figure 3.7 shows a schematic of the electro-spinning machine set-up.

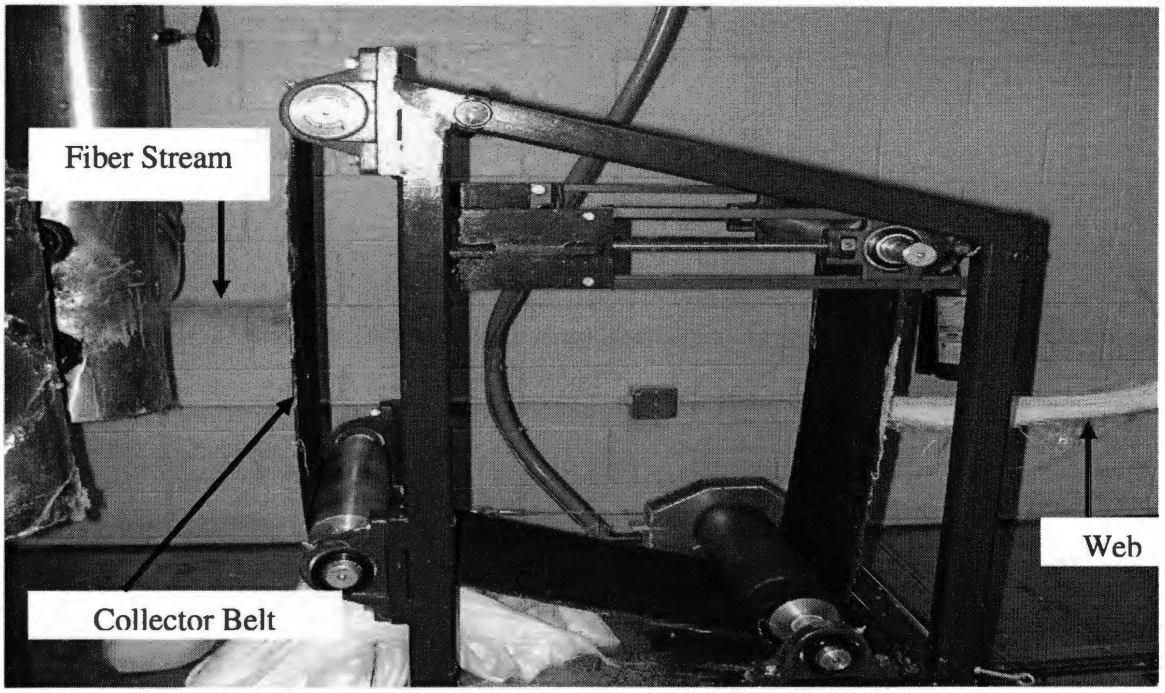

(a)

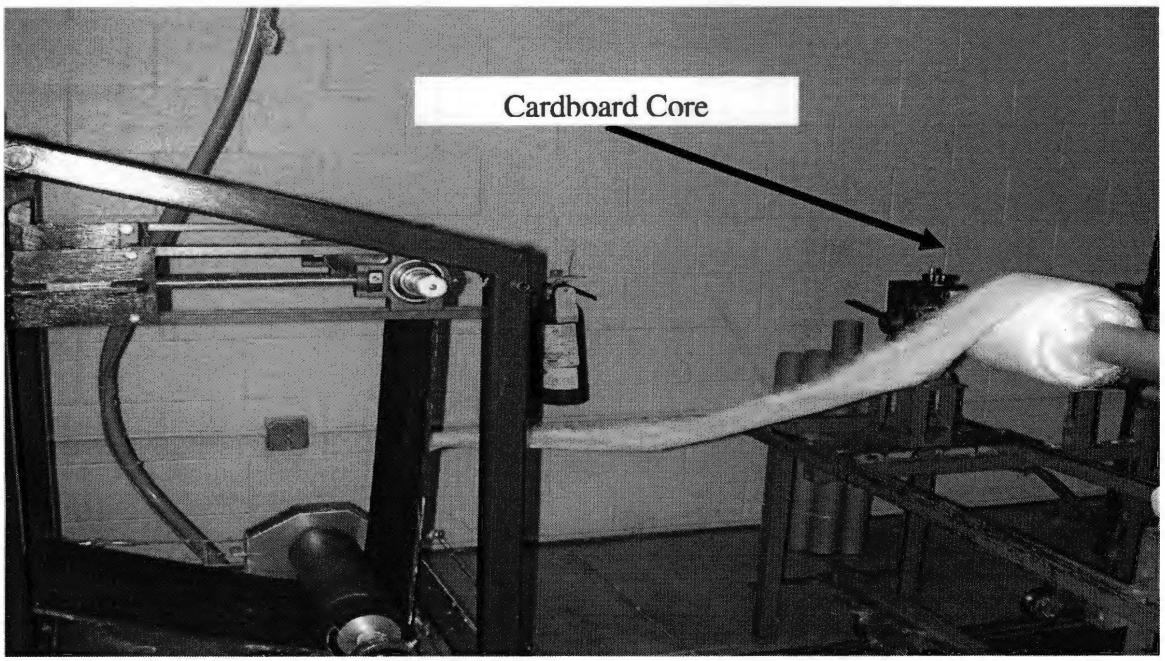

(b)

Figure 3.6: Melt-blowing collector system: (a) conveyor collector for fiber leaving the die assembly and (b) cardboard collector for nonwoven material leaving conveyor collector.

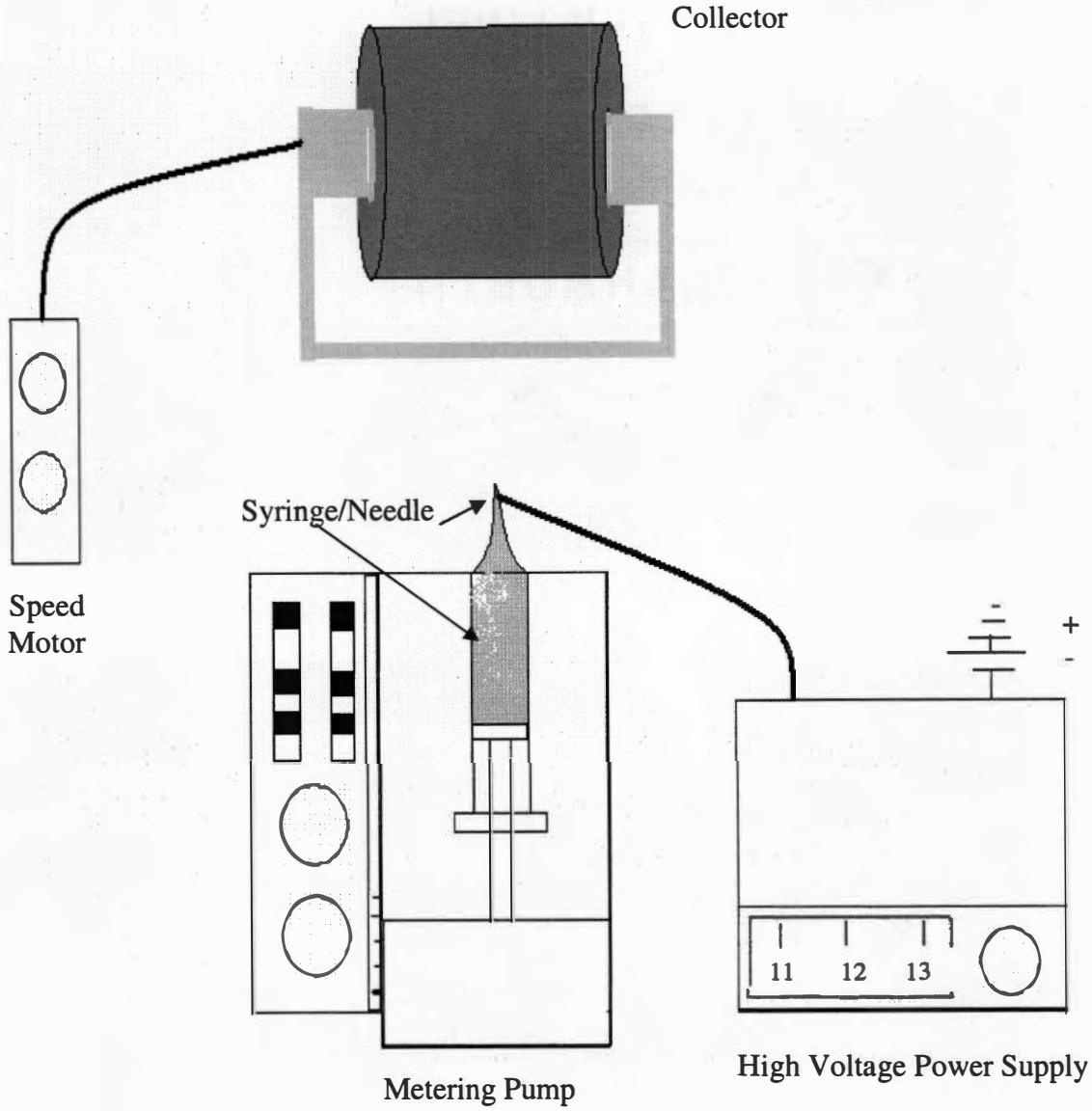

Figure 3.7: Schematic of electro-spinning machine set-up.

A. Electro-spinner Nozzle

The first part of the electro-spinning machine was an electro-spinner nozzle and it is one of the most important parts of the electro-spinning process. The nozzle consists of a 10ml latex free Luer-Lok syringe and a 20G1 precision glide needle. The syringe and needle were used in unison along with a polymer solution. The syringe held approximately 10ml of the polymer solution, which was forced out of the needle. A Sage Thermo Orion metering pump provided the force needed to push the polymer solution out of the syringe. For this research, the pump forced 10ml of solution out of the needle at a rate of 0.01ml/sec or 10ml/hr. If the rate increased, then shot or globules formed.

B. Power Source

The Second part of the electro-spinning machine is a power source. In order to form fibers it is necessary to use a voltage power source, which is connected to the needle and also grounded. The power source used was a high voltage power supply that used approximately 12 kV to charge the polymer solution as it left the needle. The charging of the solution leads to the formation of fibers.

C. Web Formation

The third part of electro-spinning is the formation of the fiber webs. Once the force is applied to the syringe, the polymer solution is slowly forced thru the needle where it is then charged. When the voltage potential exceeds the surface tension of the liquid droplet at the end of the needle, the fibers are rapidly drawn toward the grounded collector. As the solution leaves the needle, an exhaust fan is then used to evaporate the solvent contained in the solution and also to guide the fibers towards the web collector.

The fibers are laid onto a rotating collector forming a nonwoven web that is self-bonded. The laying of the fibers is due to the spraying motion that occurs as the polymer solution leaves the needle.

D. Web Collectors

The web collector is the final part of the electro-spinning process. The purpose of the web collector is to collect the fiber webs after they have solidified. For this research, there were two collectors. The first collector was a cylindrical aluminum drum that rotated. The aluminum drum was covered by a sheet of collector paper that was placed around the center of the drum in order to collect the fiber webs. The second collector was a long thin copper rod that rotated and was partially covered by a 4mm stainless steel spring. Each collector used a motor to rotate the collector. As the collectors were rotated, the fiber webs were wound onto the drum or spring. Later, the sheet of paper and spring were removed along with the webs so that the webs could undergo further processing and testing. Figure 3.8 shows the collector system.

3.3 Characterization Techniques

After the polymer was melt blown and electro-spun into nonwoven web sheets and web coated springs, the samples underwent analysis. The analysis consisted of porosity, tensile strength, and SEM testing. The purpose of the tests was to help determine which web material would inhibit VSMC migration and activate new platelet growth.

A. Differential Scanning Calorimetry

The differential scanning calorimeter (DSC) was used to measure the melting temperatures of the polyether TPU, polyester TPU, and aliphatic PC TPU unprocessed

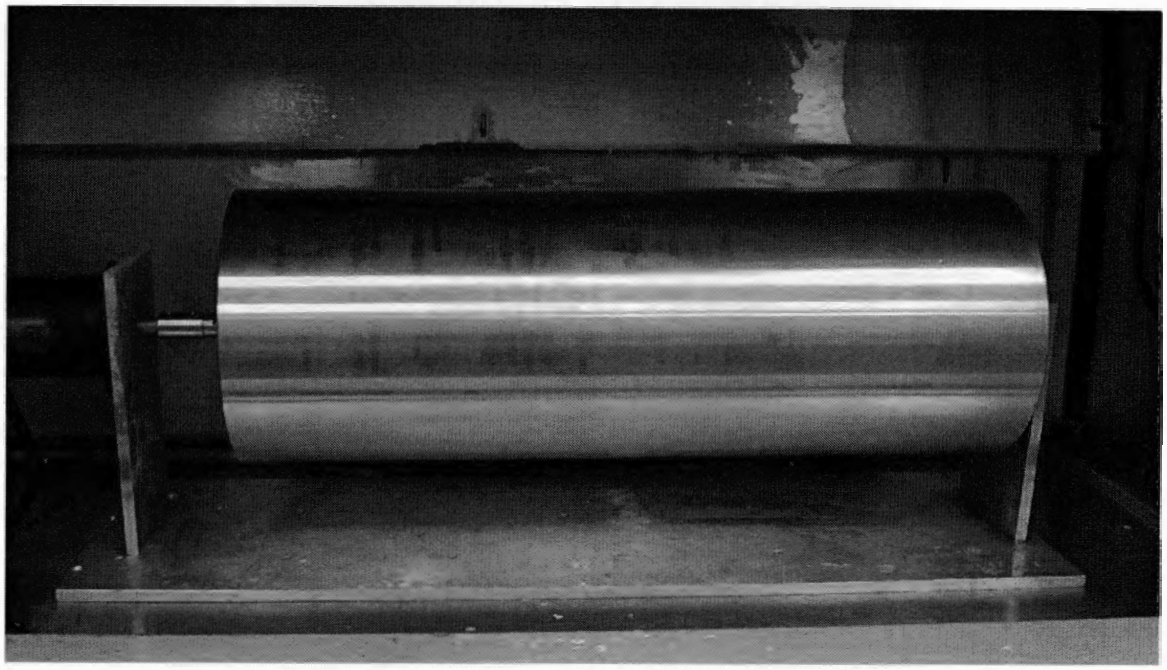

(a)

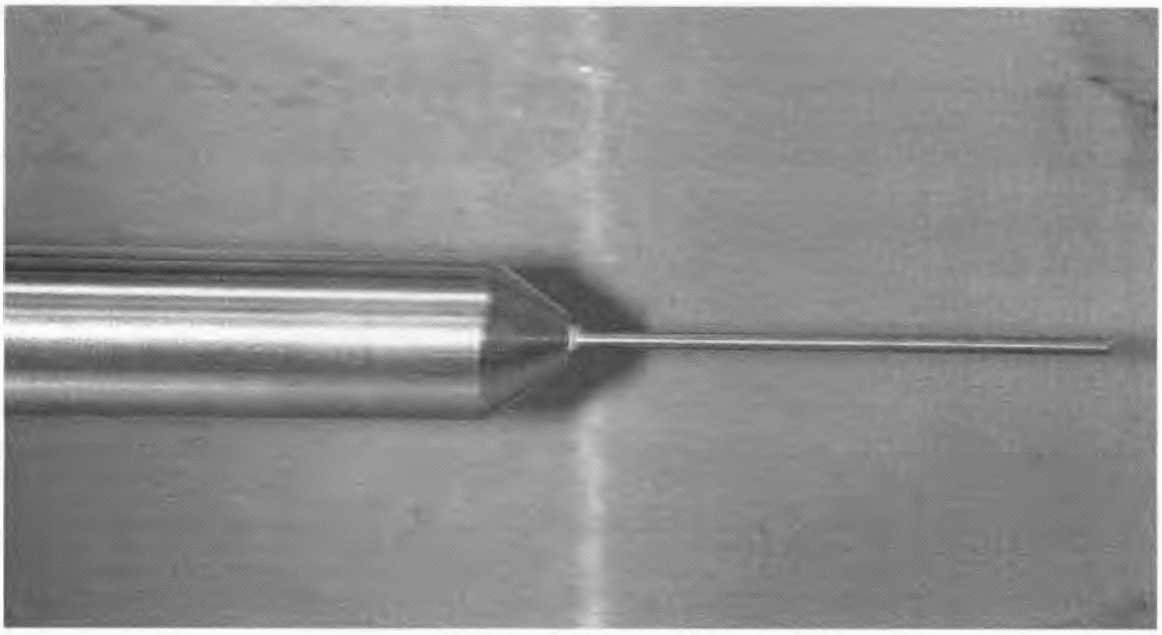

(b)

Figure 3.8: (a) Aluminum drum collector and (b) copper rod collector.

polymers. The samples were placed in a standard aluminum pan, which was weighed accurately up to 0.1 mg and placed in the DSC chamber. Before testing, the DSC machine was calibrated using a 6.2 mg indium standard at a temperature range of 120-180 °C at 10 °C/min. The melting temperature of the indium standard was 158 °C. After calibration was complete the three different TPUs underwent DSC testing in order to determine their melting temperatures. Polyether TPU and aliphatic PC TPU were both run at a temperature range of 35 °C to 400 °C at 20 °C/min., while polyester TPU was run at a range of 25 °C to 400 °C at 20 °C/min.

A plot of differential power of heat flow versus temperature was produced and analyzed for each polymer after scanning was complete. The curve was analyzed based upon their temperature peaks. Some polyurethanes do not completely melt due to the hard segments, the melting temperatures determined from testing are those of the soft-segmented parts of the polyurethanes. However, the polymers used in this research were thermoplastic polyurethanes, which allows them be melt processable.

B. Porosity (PMI)

The porosity tests were performed on a capillary flow porometer obtained from Porous Materials, Inc. The capillary flow porometer provided a fully automated through-pore analysis including mean pore size, mean pore pressure, and the standard deviation of the pore diameter. In order to perform the porosity test "a fully wetted web sample is placed in the sample chamber and sealed. Gas is then allowed to flow into the chamber behind the sample. When the pressure reaches a point that can overcome the capillary action of the fluid within the largest pore, the maximum pore diameter has been found. After determination of the maximum pore diameter, the pressure is increased and the

flow is measured until all pores are empty, and the sample is considered dry" [33]. Then the results are displayed by the PMI software and analyzed in order to determine if and which samples had pores small enough to impair VSMC migration.

C. Tensile Strength

The tensile strength tests were performed using an Economy SSTM Series and a Multi-Station Model MS Series tensile testing machines from United Testing Systems, Inc. The Economy SSTM series was loaded with 10 lb grips and is designed as a computer inclusive, electromechanical, test system. The Multi-Station Model MS Series uses pneumatic gripping systems, clamping extensometry devices, strain gage load cells, and sample measuring devices to test the materials [35]. The web samples used in the Economy SSTM series machine were a 1" by 6" cut samples that were placed into the grips that were 2 inches apart. The Multi-Station Model MS Series machine used samples that were cut 1" by 8" and placed in the grips that were 5 inches apart. All the samples were stretched to their breaking points and the results from the tests were displayed by United Testing, Inc software and analyzed based upon the forces applied and the elongation sustained by each web sample.

D. Scanning Electron Microscopy (SEM)

SEM was used to evaluate the fiber diameters of the melt blown and electro-spun webs. SEM is an electron microscope that is capable of producing surface images through the use of high resolution. The SEM consists of an electron gun, vacuum column, condensing lens, scan coils, objective lens, electron beam, secondary electrons, a detector and amplifier, the target sample, and a computer. Before the melt blown and electro-spun

samples could be placed into the microscope, they first had to be dried and sputter coated with gold using a sputter coater machine [36].

Once the SEM captured the photographs of the specimens, then Image Pro Plus was used to analyze the photographs. The Image Pro Plus software was used because of its ability to process images acquired by SEM. The software was not only able to capture and process single images but also sequences of images in grey scale. The grey scale ran at 8 bits. The software also allowed the images to undergo enhancements. The enhancements used were that of sharpening and softening of the images, which prepared the images to undergo measuring. The measurements obtained were that of the fiber diameters of the melt-blown and electro-spun samples. Figure 3.9 shows an example of two different SEM images, one melt-blown web and one electro-spun web, used with the Image Pro Plus software [36].

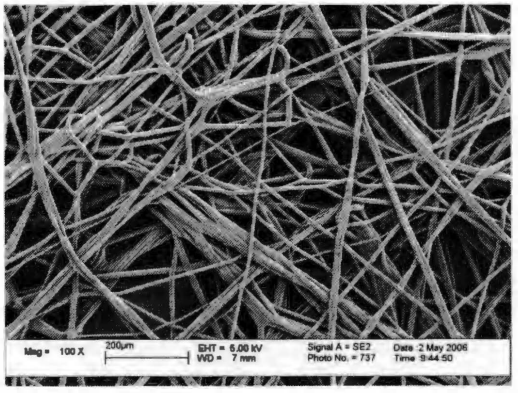

(a)

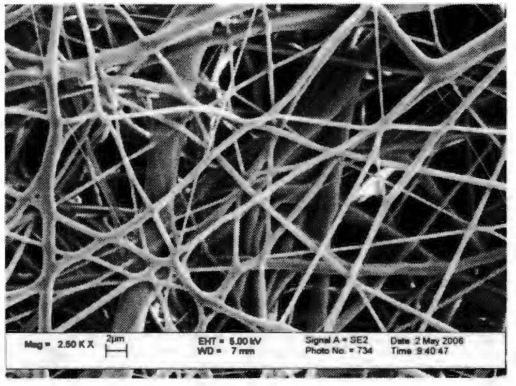

(b)

.Figure 3.9: (a) Melt-blown photos produced by Image Pro Plus software and

(b) electro-spun photos produced by Image Pro Plus software

IV. Results and Discussion

4.1 Materials Selection and Preparation

In order to choose the appropriate polymer that could be used for a biomedical application hemocompatibility and biocompatibility must first be considered. Hemocompatibility is when the materials allow the device to function while in contact with blood without causing adverse reactions. Biocompatibility is when the materials and their degradation products do not elicit adverse responses within the body [24].

The polyurethanes chosen for this study were an polyester-based thermoplastic polyurethane (TPU), a polyether-based thermoplastic polyurethane (TPU), and an aliphatic polycarbonate (PC)-based thermoplastic polyurethane (TPU) with the latter designed for extended use in the body [37]. The polyether TPU was not originally designed for medical use. However, the properties of the polymer allowed it to obtain FDA approval, which meant that this polymer could be used for an implantation device [38]. Unlike the aliphatic PC TPU, the polyester TPU was not specifically designed for medical grade applications. The beneficial properties of polyester TPU are that there are no adverse internal effects and it has rubber-like characteristics as a highly elastic compound with a good recovery [39].

Once the polyurethanes were selected for this research study, they were dried in a desiccator for 24 hours in order to remove unwanted moisture. The polyether TPU and the aliphatic PC TPU were used in the melt blowing process. The polyester TPU and aliphatic PC TPU were used in the electro-spinning process.

The selected polymers were dried overnight at 105°C in a Conair dessicant dryer and kept dry until they were added into the melt-blowing machine. For both the MB

polymers, the machines melting temperature was run at 450°F. It was found that if the temperatures were set too high the melted polymer would not form fiber webs but small fiber-like beads. After melting, the polymers formed nonwoven webs onto the collector and were wound up onto 3inch I.D. cardboard tubes. Kraft paper was rolled up with the webs in order to avoid distorting the webs and to prevent the layers of webs from sticking together. There were three tubes collected for the polyether TPU and two tubes for the aliphatic PC TPU of different weights and thicknesses.

As for the electro-spun polymers they were combined with 85 ml of DMF and 85 ml of THF for different concentrations that were heated and mixed for at least 2 hours. There were two set of solutions made. The first set consisted of 15wt% polyester TPU and 15wt% aliphatic PC TPU. The second set consisted of eight different solution concentrations made up of 5 wt%, 10 wt%, 15 wt%, or 20wt% of the two polyurethanes as listed in Table 4.1. Each set was made for different purposes. The first set was made for electro-spinning into flat sheets. The second set was made to be electro-spun onto flat web sheets of the pre-made melt-blown nonwoven webs. They were a total of 8 solutions made and 24 sets of web sheets formed, which were divided up as listed in Table 4.1.

4.2 Characterization Techniques

A. Differential Scanning Calorimetry

Differential scanning calorimetry (DSC) tests were performed in order to determine the melting temperatures of the polyurethanes. Figures 4.1, 4.2, and 4.3 show the DSC results for all three polyurethanes, along with their corresponding identification numbers. The tests revealed that polyether TPU (58245) had a melting temperature (Tm)

Table 4.1: ES samples concentrations and amount of materials.

Polymer Type	Identification Label	Solution Concentration (wt%)	Number of web samples made
Polyester TPU	EP1, EP2	15	4 flat sheets
Aliphatic PC TPU	EA1, EA2	15	4 flat sheets
Polyether TPU MB covered with ES polyester TPU	MEP1 MEP2 MEP3	5 10 15 20	3 flat sheets for each wt% for a total of 12 flat sheets
Aliphatic PC MB covered with ES aliphatic PC TPU	MEA1 MEA2	5 10 15 20	2 flat sheets for each wt% for a total of 8 flat sheets

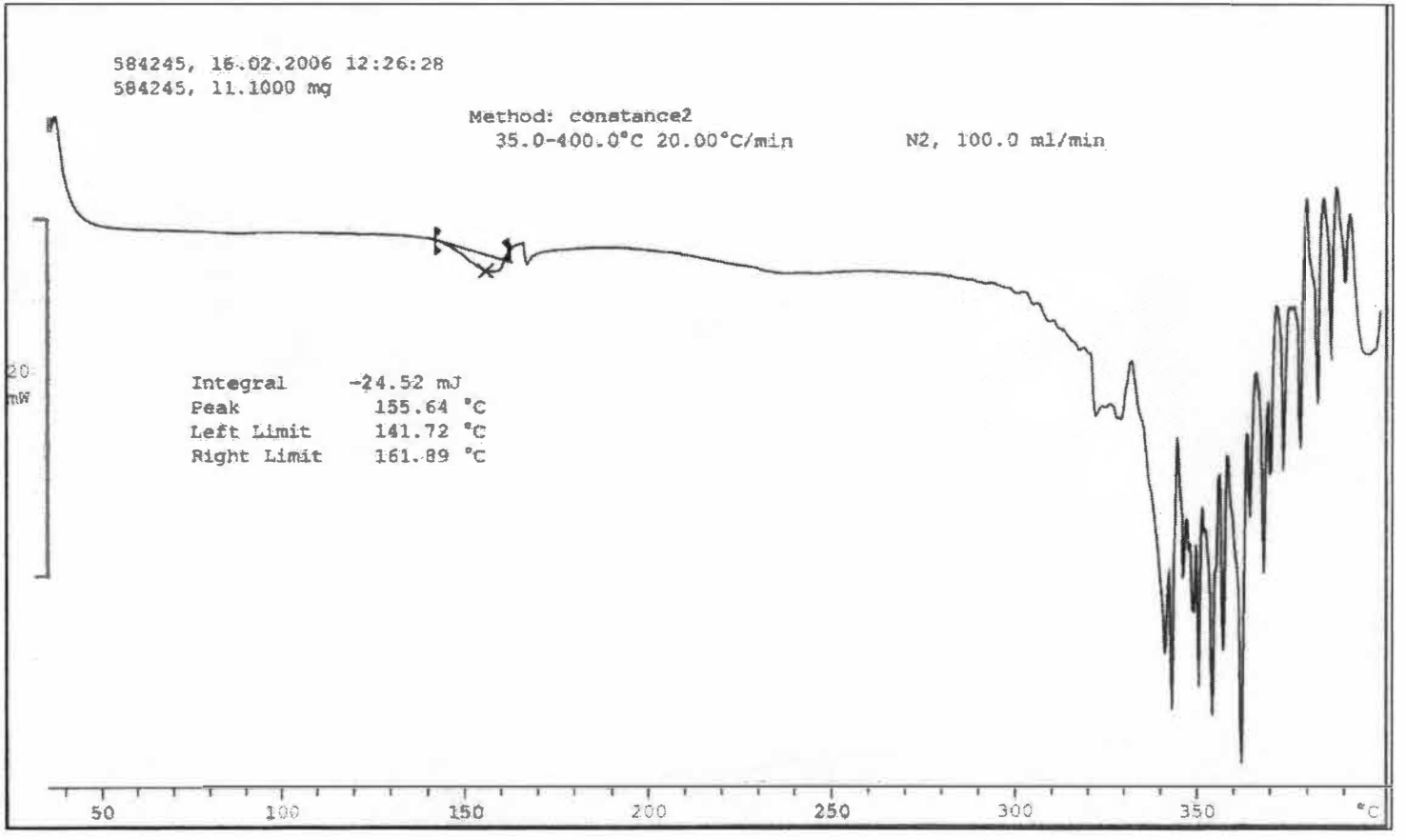

Figure 4.1: Plot of DSC for polyether TPU.

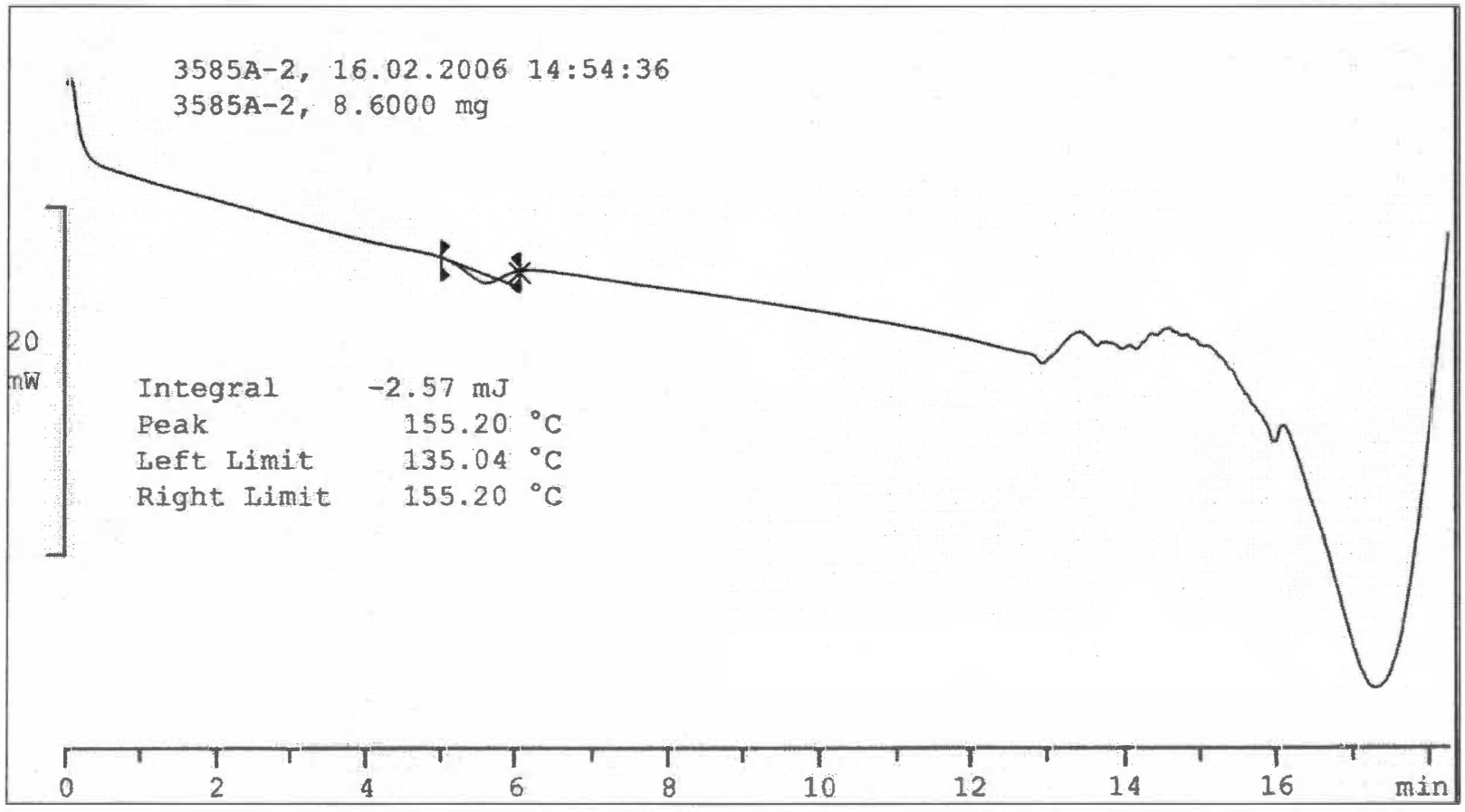

Figure 4.2: Plot of DSC for aliphatic PC TPU.

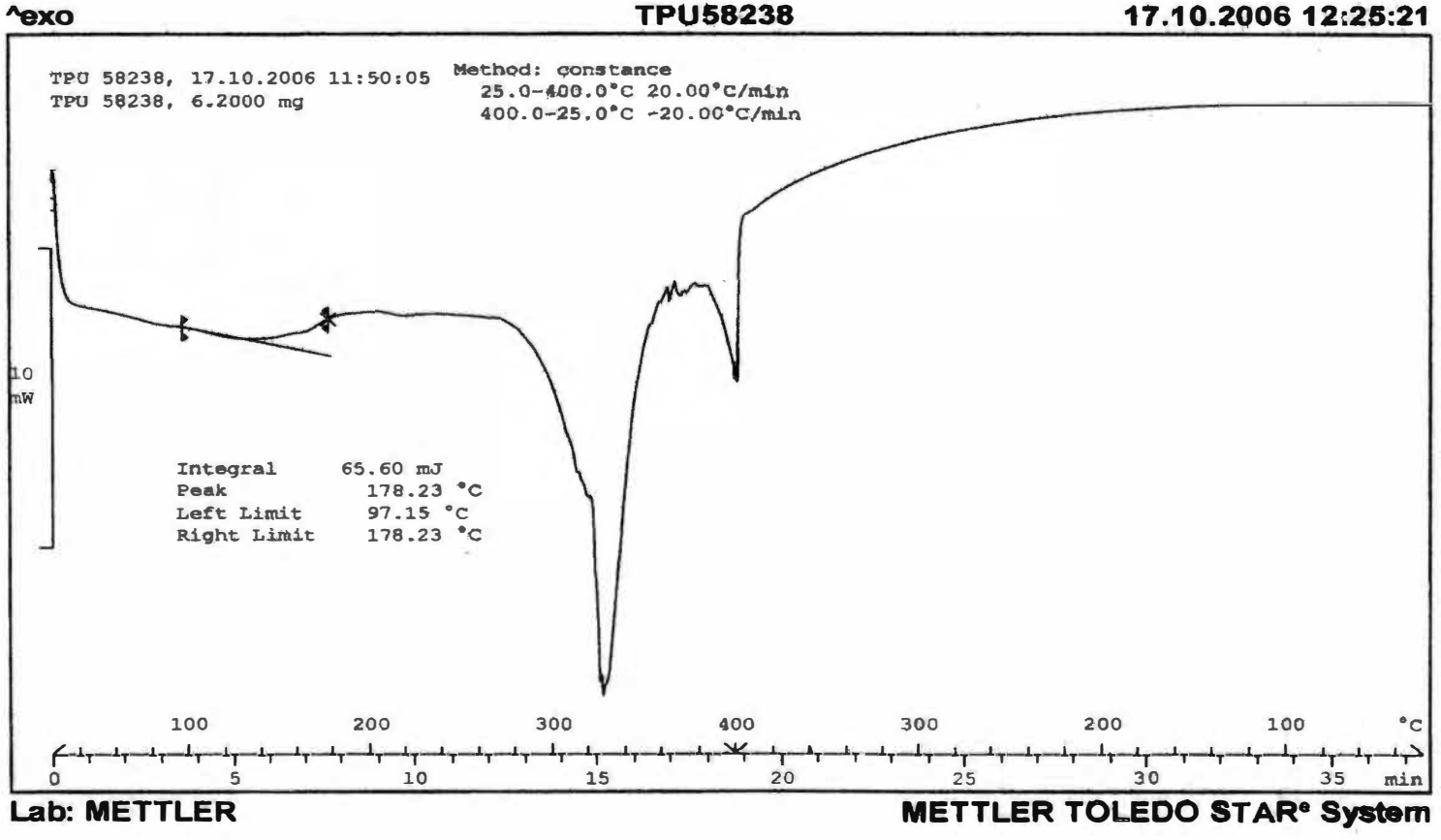

Figure 4.3: Plot of DSC for polyester TPU.

of 156 °C, which was close to the temperature in Zapletalova's study on melt blown polyether TPU of 160 °C [40]. The aliphatic PC TPU (3585A) showed a T_m of 155 °C, which is different than Noveon's findings of 193 °C to 223 °C [41]. The polyester TPU (58238) showed a T_m of 178 °C, which is also different from other findings of 215 °C [42]. The differences in the polyurethanes melting temperatures from other findings are due to their morphologies with respect to the soft and hard segments. If the length of the hard segment increases, the melting temperature increases making it harder to melt the polymer. The polyurethanes used in this research were thermoplastic which contained soft segments and hard segments that resulted in low melting temperatures.

B. Porosity Testing

Porosity is what determines the rate that human tissue will grow and encapsulate the implant. So, the tests were performed in order to determine which polyurethane web would better filter out vascular smooth muscle cells (VSMC). An attempt was made to produce mean pore diameters of 10 μm or less. In order to perform the porosity tests, pieces of each of the different web sheets of MB and/or ES webs were cut into two or three small square samples, approximately 5 in^2 pieces. They were each then weighed and measured for thickness, based upon ASTM D5729 standard, before placement into the PMI machine. The machine used was a capillary flow porometer from Porous Materials, Inc, which used a cylindrical disk that contained a 0.8 cm diameter hole at the center of the disk. The 0.8 cm diameter hole was used in order to allow air to flow through the samples. After the samples were placed into the porometer, they were slightly wetted with Salwick solution in preparation of a wet flow/dry flow test. The wet flow/dry flow test first tested the webs as wet, then as a dry.

The first set of web sheets tested were that of the MB polyether TPU and aliphatic PC TPU, summarized in Table 4.2. The table shows the mean pore diameters and pressures, weights, and thicknesses of the samples. In the top portion of the table it shows the results for the polyether TPU and the bottom portion for the aliphatic PC TPU. Since the mean pore diameters ranged from 18.9 to 30.6 μm, the MB polyether TPU and aliphatic PC TPU pore diameters that were considered too large.

As for the ES polyether TPU and aliphatic PC TPU web sheets tested, the porosity results summarized in Table 4.3 show that both types ES webs could possibly impair cellular migration. The table shows that the web sheets had mean pore diameters ranging from 3.5 to 9.1 μm, which should impair migration of through the materials. In the end, the porosity results show that between the MB and ES webs, that electro-spinning produces webs with much lower pore sizes.

Knowing the porosity results of the MB and ES materials, the next step was to combine the two methods and form an MB and ES composite. Different weights of MB webs were coated with ES webs spun from different concentrations ranging from 5 to 20 wt%. The porosity results for the MB polyether TPU and ES polyester TPU are shown in Table 4.4. The results show that the three different thicknesses of 15wt% polymer concentration of the composite MB polyether TPU with ES polyester TPU have mean pore diameters in the range of 3.7 to 6.7 μm, which is less than 10 μm. The table also revealed that the thicker 20wt% polymer concentration also met the pore diameter requirement of 10 μm with pore diameters of 7.9 μm. The other two samples had pore diameters ranging from 16 to 31.5 μm, which are considered too large. So, both the MB polyether TPU with ES 15wt% concentration polyester TPU and the MB polyether TPU

Table 4.2: MB polyether TPU and aliphatic PC TPU porosity results.

Material	Thickness (mm)	Weight (g)	Mean Pore Diameter (μm)	Mean Pore Pressure (psi)	Standard Deviation of Pore Diameters (μm)
M1 Polyether TPU	0.10	0.04	30.6	0.21	2.1
M2 Polyether TPU	0.07	0.04	34.7	0.20	13.0
M3 Polyether TPU	0.11	0.07	18.9	0.36	4.4
A1 Aliphatic PC PU	0.09	0.02	33.2	0.13	3.7
A2 Aliphatic PC PU	0.19	0.07	29.3	0.23	5.9

Table 4.3: Porosity testing results for ES polyester TPU and aliphatic PC TPU.

Material	Thickness (mm)	Weight (g)	Mean Pore Diameter (μm)	Mean Pore Pressure (psi)	Standard Deviation of Pore Diameters (μm)
EP1 Polyester TPU	0.03	0.04	3.59	1.81	0.29
EP2 Polyester TPU	0.05	0.03	5.37	1.25	1.7
EA1 Aliphatic PC PU	0.04	0.03	9.07	0.78	2.8
EA2 Aliphatic PC PU	0.02	0.01	7.39	0.64	1.3

Table 4.4 Porosity testing results for composite MB polyether TPU with ES polyester TPU.

Sample	Concentration (wt%)	Thickness (mm)	Weight (g)	Mean Pore Diameter (μm)	Mean Pore Pressure (psi)	Standard Deviation of Pore Diameters (μm)
M1	5	0.15	0.15	29.7	0.22	3.7
M2	5	0.09	0.11	31.5	0.21	4.1
M3	5	0.11	0.22	20.1	0.35	7.1
M1	10	0.14	0.13	31.3	0.21	2.9
M2	10	0.12	0.09	26.8	0.24	2.9
M3	10	0.12	0.17	20.2	0.33	3.1
M1	15	0.11	0.10	5.65	1.30	2.2
M2	15	0.13	0.10	6.66	1.10	3.0
M3	15	0.11	0.17	3.72	1.29	0.78
M1	20	0.14	0.13	7.90	0.66	7.3
M2	20	0.12	0.12	16.4	0.43	6.5
M3	20	0.11	0.17	15.9	0.45	6.6

with ES 20wt% concentration polyester TPU have pore diameters that may better impair VSMC migration As for the 5wt% and 10wt% concentrations, they are not useable because their pore diameters are considered to be too large.

With respect to the composite MB aliphatic PC TPU and ES aliphatic PC TPU the porosity results in Table 4.5 showed that the 10wt% concentration of aliphatic PC TPU resulted in pore diameters of 2.7 to 6 μm, which is less than 10μm. The table also shows that the thinner sample of 15wt% aliphatic PC TPU concentration had pore diameters of 5.5 μm, which is also less than 10 μm. The thicker 15wt% concentration web sample resulted in pore diameters slightly larger than 10 μm, with diameters of 10.7 μm. The other concentrations and web samples resulted in pore diameters of 16.4 to 20.6 μm, which were too large. So, with respect to the composite melt blown and electro-spun aliphatic PC TPU, the results show that the 10wt% concentration would better impair VSMC migration.

After performing the porosity tests on the MB, ES, and the composite MB and ES webs, they were not only analyzed separately but also together. Individually the porosity results showed that the ES and composite MB and ES web samples resulted in webs that could inhibit VSMC migration. Unfortunately, the porosity tests alone could not determine which web would better inhibit VSMC migration. Other tests were needed to make that decision.

C. Tensile Strength

There were six specimens cut from each of the melt-blown web sheets, and six specimens cut from the 28 composite MB and ES web sheets. The four electro-spun web

Table 4.5: Porosity testing results for composite of MB and ES aliphatic PC TPU.

Sample	Concentration (wt%)	Thickness (mm)	Weight (g)	Mean Pore Diameter (μm)	Mean Pressure (psi)	Standard Deviation of Pore Diameters (μm)
A1	5	0.16	0.07	12.0	0.79	8.8
A2	5	0.15	0.10	18.1	0.37	3.5
A1	10	0.25	0.09	5.99	1.09	0.65
A2	10	0.33	0.12	2.71	2.53	0.74
A1	15	0.19	0.10	5.49	1.19	0.67
A2	15	0.28	0.18	10.7	0.72	5.8
A1	20	0.25	0.07	20.6	0.32	2.8
A2	20	0.27	0.11	16.4	0.40	2.4

sheets not cut were from the set that included the 15wt% polyester TPU and aliphatic PC TPU because the web sheets were too thin to cut and stay in 1" by 6" strips. The materials underwent tensile strength tests in order to determine which materials had high strength because in order for a material to inhibit VSMC migration it must be strong enough to withstand the stress of blood flow.

Once the samples were in the testing grips they were stretched to their failure points. Tables 4.6 and 4.7 show the tensile strength results for the MB polyether TPU and the composite of MB and ES web sheets . The tables summarize the materials peak force, peak elongation %, break force, break elongation %, weight, and thickness. The peak force and peak elongation % show the point where each sample began to have breaking of the fibers in the materials. The break force and break elongation % show where the web samples had final breaking of the fibers.

In table 4.6, the MB polyether TPU samples thicknesses correspond to the peak forces and break forces the material can maintain before breaking. When the thicknesses of the samples increase from 0.05 to 0.13 mm, the peak forces increased from 0.20 to 0.57 lbs, and break forces increased from 0.07 to 0.57 lbs. The percent elongation of the MB polyether TPU samples do not increase or decrease with respect to the thickness of the samples. However, the results did show the highest peak forces and break forces had the highest percent elongation of the samples. Table 4.6 also includes the MB aliphatic PC TPU samples. It was determined that the MB aliphatic PC TPU does not act the same as the polyether TPU. As the thicknesses of the aliphatic PC TPU samples increase from 0.11 to 0.17 mm, the peak forces were approximately 0.45 to 0.43 lbs and the break forces stay the same at 0.37 lbs. The percent elongation of the samples showed that the

Table 4.6: Tensile testing results for the MB materials.

Sample	Weight (g)	Thickness (mm)	Peak Force (lbs)	Peak % Elongation	Break Force (lbs)	Break % Elongation
M1	0.11	0.11	0.31	924	0.24	1118
M2	0.11	0.05	0.2	1080	0.07	1128
M3	0.21	0.13	0.57	1226	0.57	1234
A1	0.14	0.11	0.45	1086	0.37	918
A2	0.19	0.17	0.43	950	0.37	988

Table 4.7: Tensile testing results for composite MB and ES materials.

Sample	Polymer Concentrations (wt%)	Weight (g)	Thickness (mm)	Peak Force (lbs)	Peak % Elongation	Brea k Force (lbs)	Break % Elongation
A1	5	0.14	0.16	0.67	222	0.44	235
A2	5	0.16	0.15	0.49	207	0.22	231
A1	10	0.18	0.25	0.47	194	0.24	208
A2	10	0.2	0.33	0.65	165	0.38	186
A1	15	0.14	0.19	1.09	252	0.85	262
A2	15	0.16	0.28	1.42	250	1.07	258
A1	20	0.14	0.25	0.75	230	0.44	240
A2	20	0.15	0.27	0.89	212	0.64	222
M1	5	0.19	0.15	0.44	254	0.28	302
M2	5	0.18	0.09	0.49	248	0.34	277
M3	5	0.22	0.28	0.63	268	0.37	285
M1	10	0.16	0.14	0.64	315	0.63	351
M2	10	0.14	0.12	0.54	278	0.46	306
M3	10	0.18	0.12	0.63	228	0.48	233
M1	15	0.14	0.11	0.76	258	0.59	262
M2	15	0.14	0.13	0.73	247	0.42	254
M3	15	0.19	0.11	1.09	232	0.65	244
M1	20	0.16	0.14	0.88	302	0.77	329
M2	20	0.16	0.12	0.72	334	0.57	367
M3	20	0.18	0.11	1.04	263	0.95	287

Top: Composite of MB aliphatic PC TPU with ES aliphatic TPU.

Bottom: Composite of MB polyether TPU with ES polyester TPU.

samples with the highest peak forces contained the highest peak percent of elongation. As for the break forces, which were the same, the percent elongation showed that the 0.17 mm sample had the highest break percent of elongation.

Table 4.7 shows the tensile testing results for the composite MB and ES web sheets at different polymer concentrations. The top portion of the table shows the results for the aliphatic PC TPU electro-spun onto different thicknesses of melt blown aliphatic PC TPU. There were two different MB thicknesses (as shown in Table 4.6) at four different ES polymer concentrations. The bottom portion of the table shows the polyester TPU ES onto different thicknesses of MB polyether TPU.

The results of the composite of MB aliphatic PC TPU with ES aliphatic PC TPU web samples showed that for each concentration the increase in the composite samples thickness resulted in an increase in both the peak forces and break forces. The 5wt% thickness values were 0.15 and 0.16 mm, with corresponding peak force values of 0.49 and 0.67 lbs, and break force values of 0.22 and 0.44 lbs. The 10wt% thickness values were 0.25 and 0.33 mm, with corresponding peak force values of 0.47 and 0.65 lbs and break force values of 0.24 and 0.38 lbs. The 15wt % had thickness values of 0.19 and 0.28 mm, with corresponding peak force values of 1.09 and 1.42 lbs, and break force values of 0.85 and 1.07 lbs. The 20wt% had thickness values of 0.25 to 0.27 mm, with corresponding peak force values of 0.75 and 0.89 lbs, and break force values of 0.44 and 0.64 lbs. The tensile testing results indicated that for the composite of MB aliphatic PC TPU with ES aliphatic PC TPU the overall thicker web samples had higher peak forces and higher break forces.

The percent elongation for all the concentrations, on the other hand, did not

correspond to the thicknesses of the samples. The 5wt% ES concentration results showed that the thickness values of 0.15 and 0.16 mm corresponded to peak percent elongation values of 222 and 207 % and break percent elongation values of 231 and 235 %. The 10wt% ES results showed thickness values of 0.25 and 0.33 mm that corresponded to peak percent elongation values of 194 and 165 % and break percent elongation values of 208 and 186 %. The 15wt% thickness values of 0.19 and 0.28 mm corresponded to peak % elongation values of 252.2 and 249.2 % and break % elongation values of 262 and 258.2 %. The 20wt% thickness values of 0.25 and 0.27 mm corresponded to peak percent elongation values of 230 and 212 %, and break percent elongation values of 240 and 222 %. The tensile testing results indicated that for the composite of MB aliphatic PC TPU with ES aliphatic PC TPU the thicker samples had the lower peak elongation % and the lower break elongation %.

The results for the composite of MB polyether TPU with ES polyester TPU web samples shown at the bottom of Table 4.7 indicated that for the 5wt% and 10wt% samples, the thicker samples had the higher peak forces and break forces. The 15wt% and 20wt% samples showed the thinner samples had higher peak and break forces. As for the peak elongation percent and the break elongation percent, the 5wt% results show that the thicker sample had the higher peak elongation percent and break elongation percent. The 10wt% results indicated that the thicker sample had the higher peak elongation percent and the lower break elongation percent. The 15wt% results indicated that the 0.11 mm sample that weighed 0.19 g had the lowest peak elongation percent and lowest break elongation percent. The 20wt% results indicated that the thinner sample had the lowest peak elongation percent and the lowest break elongation percent.

After performing tests to determine the webs samples peak forces, break forces, peak percent elongation, and break percent elongation the results were used to calculate the stresses and strains of the samples in order to determine the tensile strengths of the samples. The tensile strength of the samples is based upon the maximum amount of tensile stress that the material can be subjected to before complete failure occurs. Table 4.8 shows the stress and strain results for the MB samples. The MB polyether TPU shows a tensile strength of 0.29 psi with an elongation length of 2.5 inches/inch. The MB aliphatic PC TPU showed a tensile strength of 0.19 psi with an elongation of 1.8 and 2.0 inch/inch. The stress strain values for the composite aliphatic PC TPU and composite polyether TPU with polyester TPU given in Table 4.9 shows similar results as the melt blown samples. The composite aliphatic PC TPU had a tensile strength of 0.21 psi with an elongation length of 1.3 inch/inch at 15wt%. The composite polyether TPU with polyester TPU had a tensile strength of 0.19 psi with an elongation length of 1.4 inch/inch at 20wt%.

After determining the tensile strengths, the results were compared to the porosity results, which revealed that the materials with low porosity did not have the highest tensile strength. The samples with the smallest pore diameters were the ES polyester TPU (3.6-5.4 μm), the composite MB polyether TPU with 15wt% ES polyester TPU (3.7-6.7 μm), and composite MB aliphatic PC TPU with ES 10wt% aliphatic PC TPU (2-5 μm). The samples with the higher tensile strength were the MB polyether TPU (0.29 psi), the composite of MB aliphatic PC TPU with 15wt% ES aliphatic PC TPU (0.17-0.21 psi) and the composite of MB polyether TPU with 20wt% ES polyester TPU (0.15-

Table 4.8: Stress-strain values of MB samples.

Sample	Break stress (psi)	Break Strain Length (in/in)
MB	Polyether TPU	and Aliphatic PC TPU
M1	0.12	2.2
M2	0.04	2.3
M3	0.29	2.5
A1	0.19	1.8
A2	0.19	2.0

Table 4.9: Stress-strain values for composite samples.

Sample	Polymer Concentrations (wt%)	Break stress (psi)	Break Strain Length (in/in)
MB ES	Composite	Aliphatic PC TPU	
A1	5	0.09	1.2
A2	5	0.04	1.2
A1	10	0.05	1.0
A2	10	0.08	9.3
A1	15	0.17	1.3
A2	15	0.21	1.3
A1	20	0.09	1.2
A2	20	0.13	1.1
MB ES	Composite	Polyether TPU	And Polyester TPU
M1	5	0.06	1.5
M2	5	0.07	1.4
M3	5	0.07	1.4
M1	10	0.13	1.8
M2	10	0.09	1.5
M3	10	0.10	1.2
M1	15	0.12	1.3
M2	15	0.08	1.3
M3	15	0.13	1.2
M1	20	0.15	1.6
M2	20	0.11	1.8
M3	20	0.19	1.4

0.19 psi). The materials with the smallest pore sizes had predominately low tensile strengths, except for the ES polyester TPU because that material was not tensile tested. The composite of MB aliphatic PC TPU with 10wt% ES aliphatic PC TPU had tensile strengths in the range of 0.05 to 0.08 psi. The composite of MB polyether TPU with 15wt% ES polyester TPU had tensile strengths in the range of 0.08 to 0.13 psi. The pore diameters of the MB aliphatic PC TPU were 29.3 to 33.2 μm and the composite of MB polyether TPU with 10wt% ES polyester TPU were 20 to 31 μm, which were too large to impair VSMC migration. The pore diameters of the composite MB aliphatic PC TPU with 15wt% ES aliphatic PC TPU were 5.5 to 10.7 μm, which could possibly inhibit VSMC migration since the pore diameters are below or close to 10 μm. In the end, the analysis of the porosity and tensile strength tests revealed that composite of MB polyether TPU with 15wt% ES polyester TPU and composite of MB aliphatic PC TPU with 15wt% ES aliphatic PC TPU materials show better properties in impairing VSMC migration because of their pore diameters and tensile strengths.

D. Scanning Electron Microscopy (SEM)

Once the porosity and tensile strengths were determined for each set of web sheets, the fiber diameters were also determined. The SEM processes captured photographs for different MB, ES, and a composite of MB and ES webs. For the MB materials, SEM was performed on the M1 and M3 polyether TPU samples and on the A1 and A2 aliphatic PC TPU samples. The M2 polyether TPU was not examined because of the large pore diameters of 34.7 μm. As for the ES materials, EP1 polyether TPU and EA1 aliphatic PC TPU samples were examined because of their porosity results. Lastly,

from the composite of MB and ES samples MEP1, MEP2, MEA1, and MEA2 were examined because each of these had good pore diameters.

After the photographs were captured they were then examined using Image Pro Plus software, which allowed for the measuring of the fiber diameters. As can be seen in Table 4.10 the MB fiber diameters were form 6 μm to 9 μm. As for the ES samples their fiber diameters ranged from 0.26 μm to 0.7 μm. Figures 4.4, 4.5, and 4.6 shows some of the photographs of the MB and ES samples. The composite of MB and ES samples fiber diameter results are summarized in Table 4.11. These results show the same trend as the MB and ES fiber diameters in that the ES fibers were smaller than the MB fibers. In some instances the photographs showed both the MB and ES fibers, which can be seen in Figures 4.6 and 4.7.

Other than using SEM to measure the fiber diameters of the samples, it was also used to obtain a better understanding of the properties of the materials. Figure 4.4 shows that the MB polyether TPU fibers were laid so that there were visibly large pores within the material. In parts (a) and (b) the right hand figures show an up close view of the left hand photo, which are an overview of the samples. Figure 4.5 showed the MB aliphatic PC TPU as closely packed laid fibers. Figure 4.6 shows polyester TPU and aliphatic PC TPU as ES fibers. These fibers were randomly laid but also contained large sections of shot for the EP1 and EA1.1 samples and little shot in the EA1.2 sample, which meant that as the material became thicker the amount of shot decreased. Figure 4.7 shows the composite of MB polyether TPU with 20wt% ES polyester TPU and the composite of MB aliphatic PC TPU with 5wt% and 15 wt% aliphatic PC TPU samples. In these

Table 4.10: Fiber diameters of the MB and ES materials.

Material	Sample	Mean Diameter (μm)	Standard Deviation (μm)
MB polyether TPU	M1	8.5	1.9
MB polyether TPU	M3	8.9	1.4
MB aliphatic PC TPU	A1	6.2	4.0
MB aliphatic PC TPU	A2	7.0	1.9
ES polyester TPU	M1	0.3	0.15
ES aliphatic PC TPU	A1	0.6	0.18

Table 4.11: Fiber diameters for the composite of MB and ES materials.

Material	Sample (wt%)	Mean Diameter (μm)	Standard Deviation (μm)
MEP1 polyether TPU/polyester TPU	10*	11	1.1
MEP1 polyether TPU/polyester TPU	15	9.9	3.2
MEP2 polyether TPU/polyester TPU	5	7.9	2.7
MEA1 aliphatic PC TPU/aliphatic PC TPU	5*	6.8	3.3
MEA1 aliphatic PC TPU/aliphatic PC TPU	5**	0.15	0.06
MEA1 aliphatic PC TPU/aliphatic PC TPU	15*	3.3	1.2
MEA1 aliphatic PC TPU/aliphatic PC TPU	15**	1.8	1.1
MEA2 aliphatic PC TPU/aliphatic PC TPU	10	0.45	0.13
MEA2 aliphatic PC TPU/aliphatic PC TPU	20	7.1	3.4

* The melt blown results for the given sample.

** The electro-spun results for the given sample.

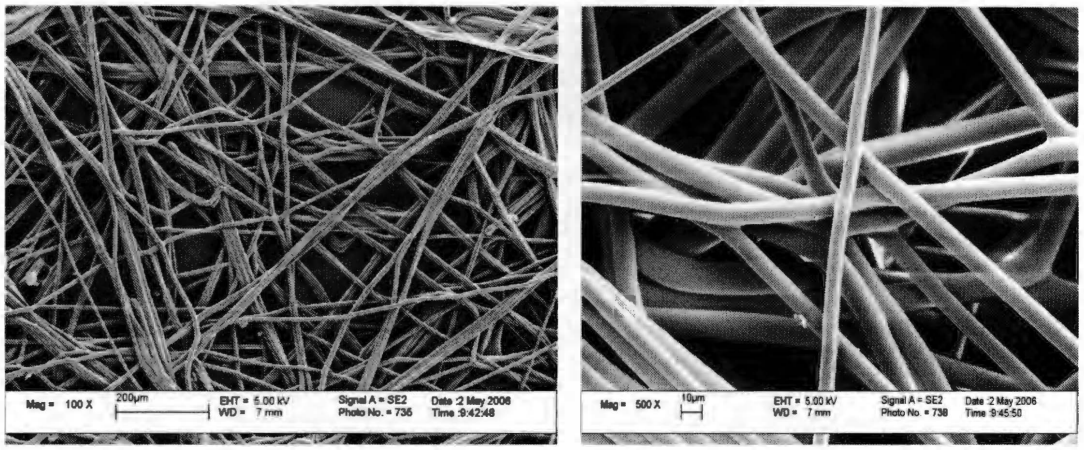

(a)

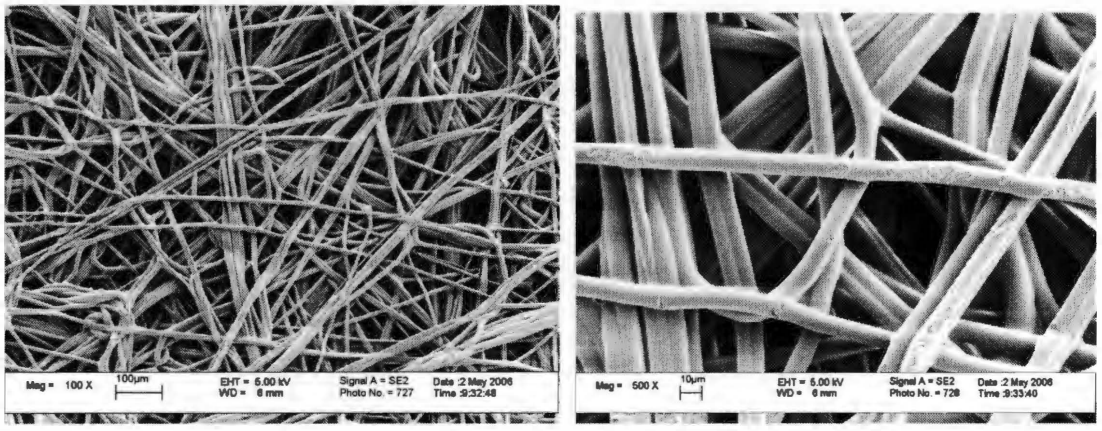

(b)

Figure 4.4: SEM photographs of melt-blown polyether TPU: (a) sample M1 and (b) sample M3.

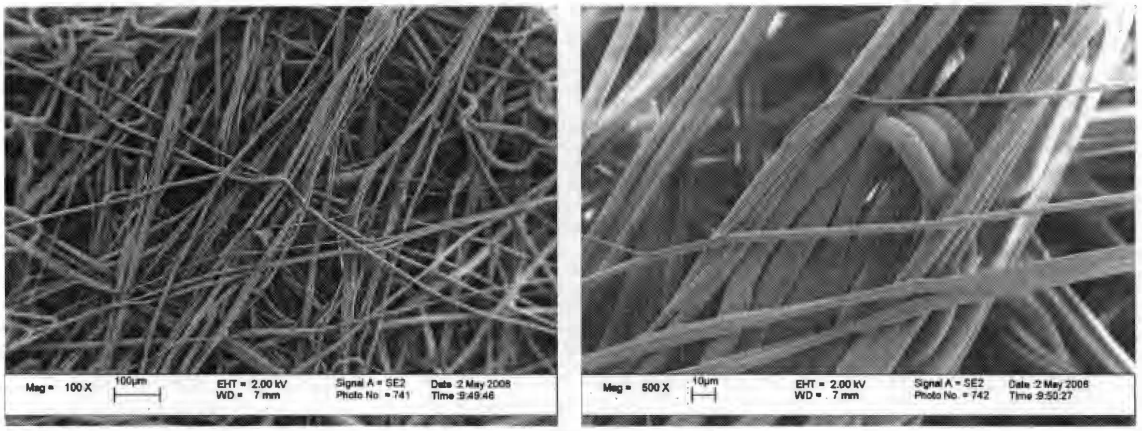

(a)

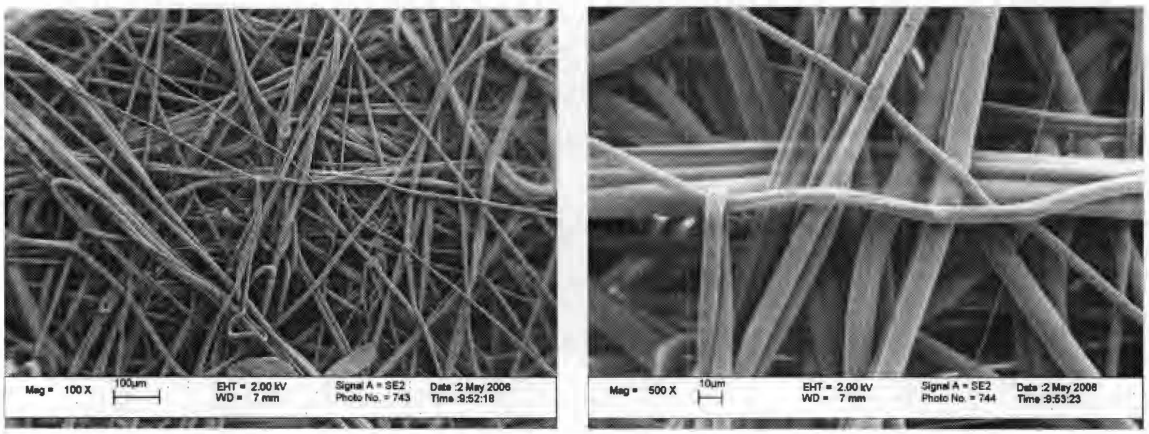

(b)

Figure 4.5: SEM photographs of melt-blown aliphatic PC TPU: (a) sample A1 and (b) sample A2.

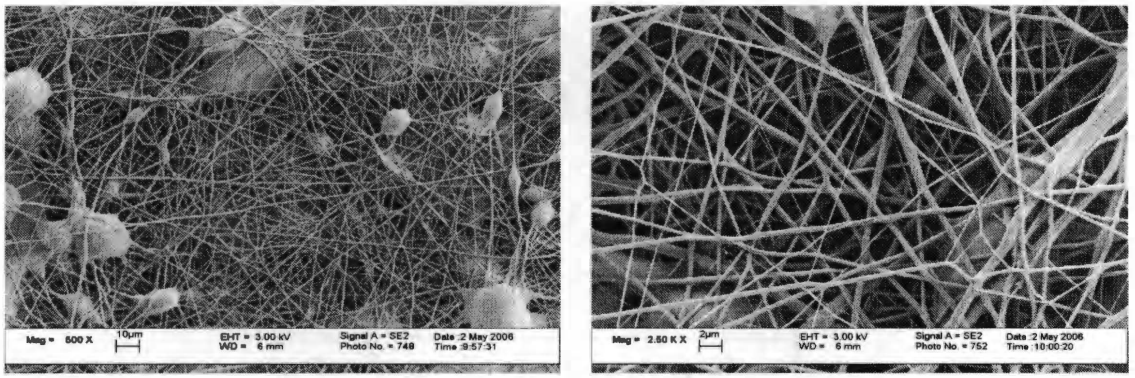

(a)

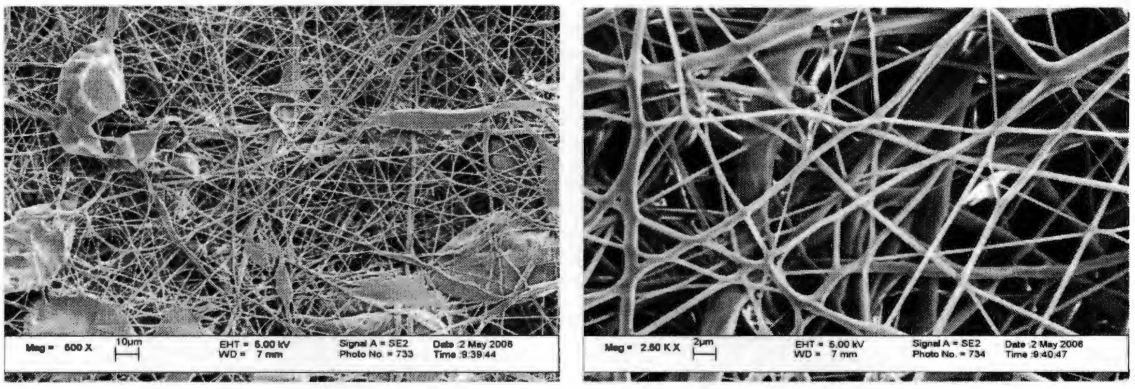

(b)

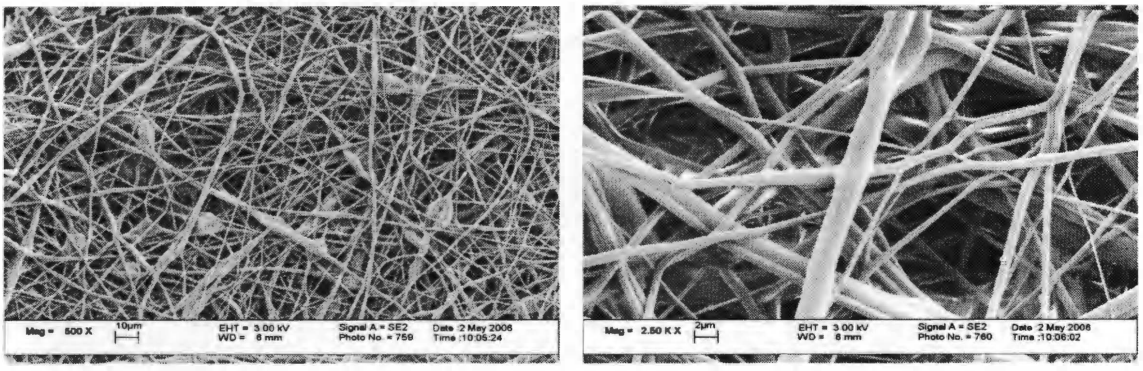

(c)

Figure 4.6: SEM photographs of electro-spun polyether TPU and aliphatic PC TPU: (a) sample EP1, (b) sample EA1.1, and (c) EA1.2.

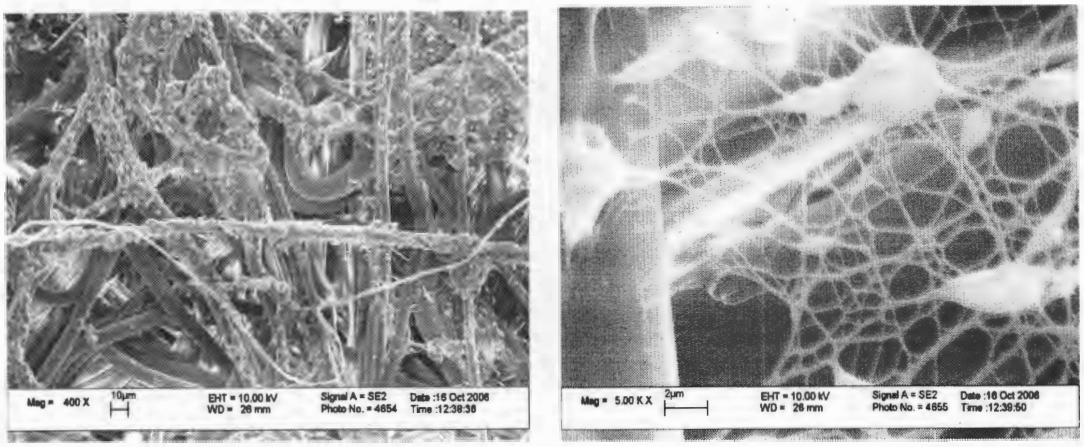

(a)

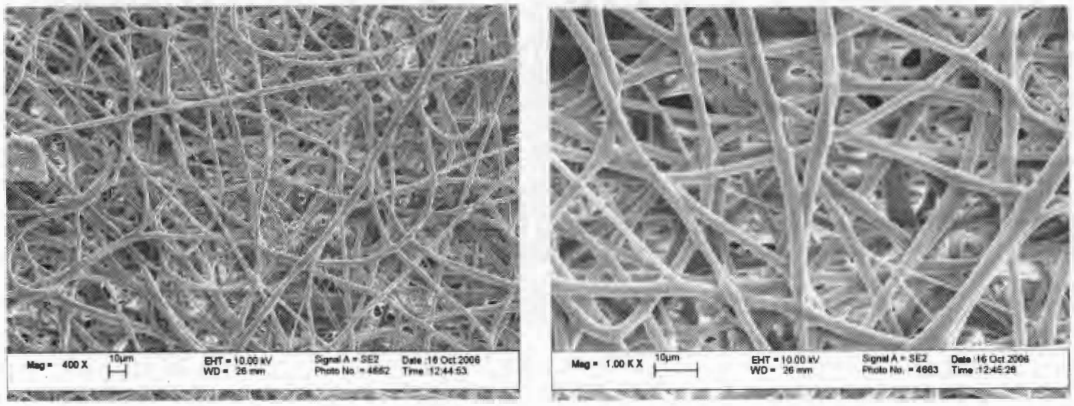

(b)

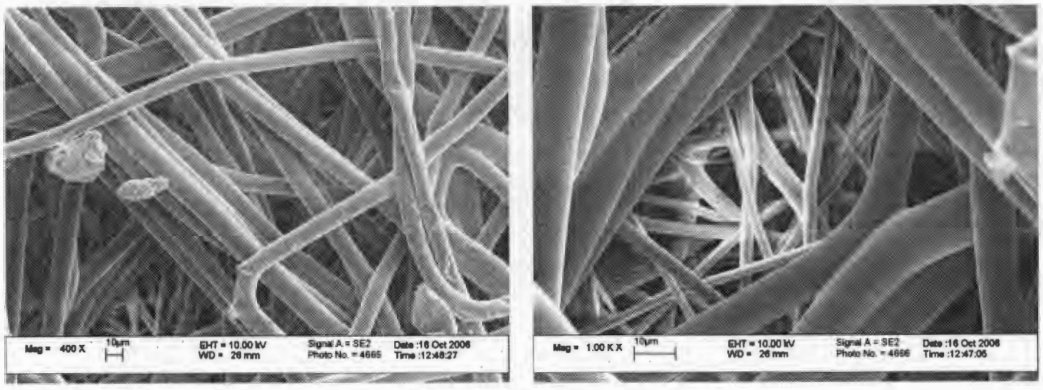

(c)

Figure 4. 7: SEM photographs of composite of melt-blown and electro-spun fibers: (a) sample MEA1 at 5wt%, (b) sample MEA1 at 15wt%, and (c) sample MEP1 at 20wt%.

photographs the fibers were laid upon each other to form tightly packed fibers. The fibers were also laid so that SEM was able to take photomicrographs of both the MB and ES fibers. The figures on the right show the MB fibers up close, while the figures on the left show the ES fibers up close. Figure 4.8 shows the composite of MB polyether TPU with ES polyester TPU fibers that do not show both the MB and ES fibers. It does, however, show that the randomly laid fibers are very tightly packed with minimal pore visibility. Lastly, figure 4.9 shows the composite of MB aliphatic PC TPU with ES aliphatic PC TPU fibers. In these samples the fibers were also randomly laid like the other samples, except that these fibers formed an extremely tight packed material that resembled sheets of thick paper. The figures on the left show a close up view of the figures on the right, which are an overview of the samples.

4.3 Fiber Coated Springs

As mentioned in section III there were two electro-spinning collectors. One was an aluminum cylindrical drum and the other a copper rod. The results discussed previously all came from webs that were formed onto the drum. However, for each set of web sheets made, springs were coated with the same web material. The copper rod allowed 4 mm diameter stainless steel springs to be rotated so that fiber webs could be formed onto the outside of the springs. The formation of the web coated springs were created not to undergo tensile, porosity, or fiber diameter testing. Instead, the springs were created for two purposes. The first purpose was to test if the electro-spun webs would adhere to the springs as a barrier. The second purpose was to take those coated springs and to perform in vivo tests along with the web sheets.

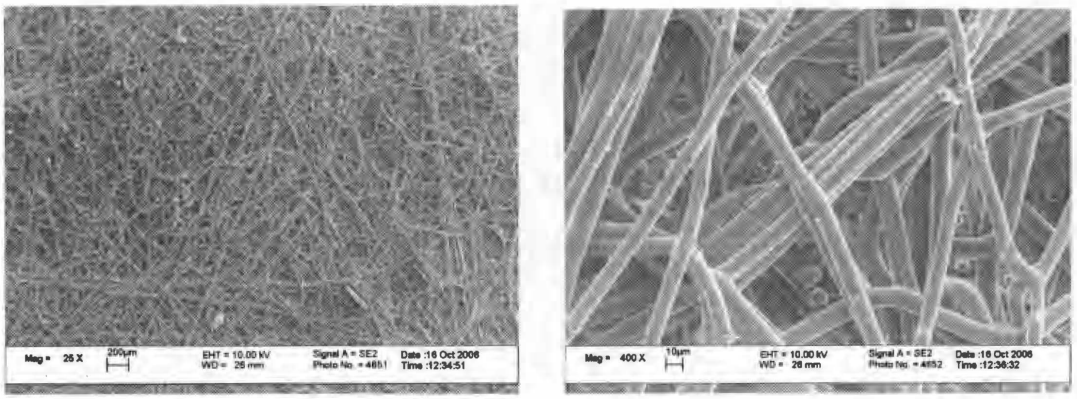

(a)

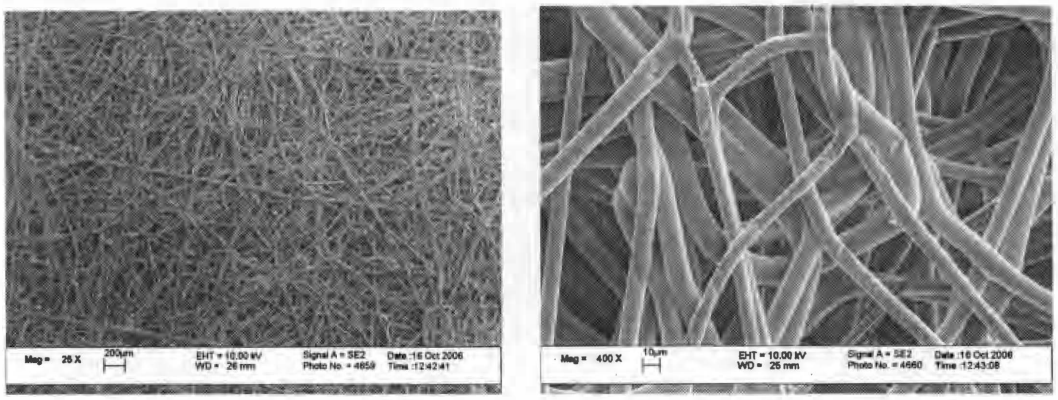

(b)

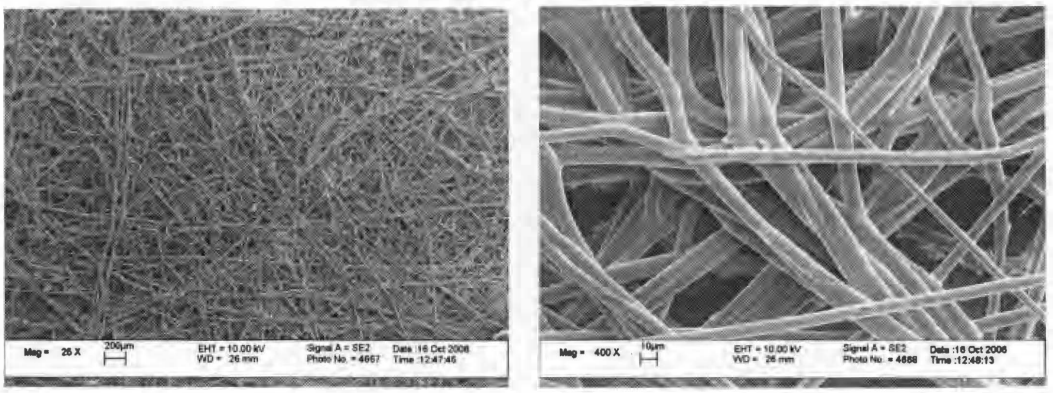

(c)

Figure 4.8: SEM photographs of the composite of melt-blown polyether TPU with electro-spun polyester TPU fibers: (a) MEP1 at 10wt%, (b) MEP1 at 15wt%, and (c) MEP2 at 5wt%.

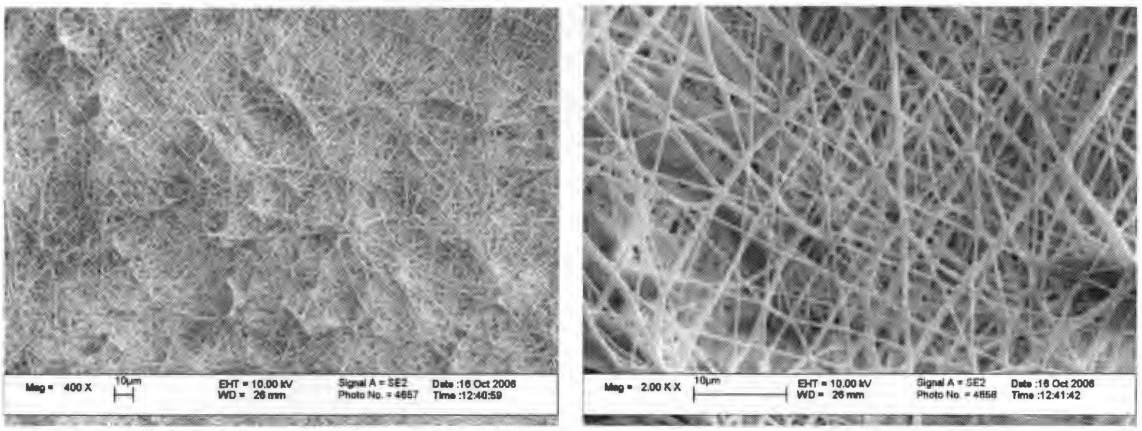

(a)

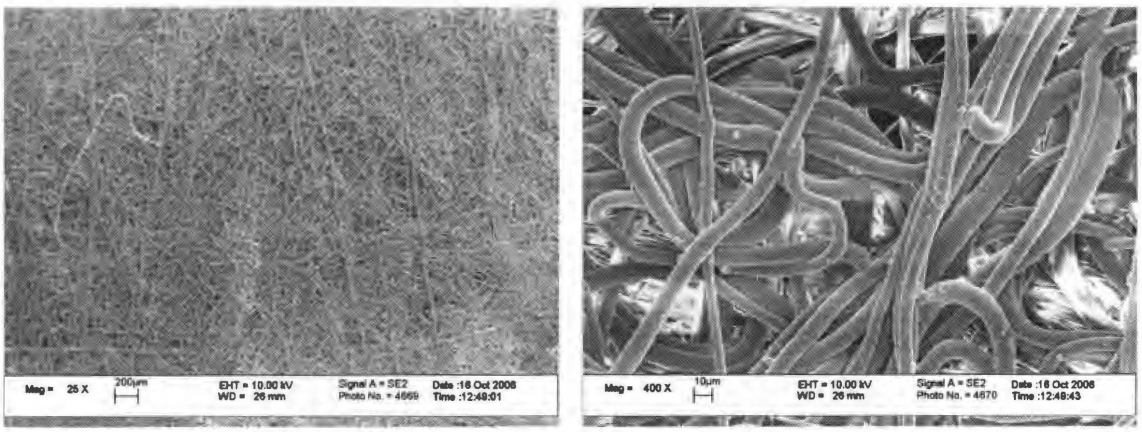

(b)

Figure 4.9: SEM photographs of the composite of melt-blown aliphatic PC TPU and electro-spun aliphatic PC TPU: (a) MEA2 at 10wt% and (b) MEA2 at 20wt%.

The first purpose was achieved because most of the polymer concentrations formed fibers onto the springs, except for the 20wt% concentration. It was determined that the 20wt% concentration was too thick for the electro-spinning process to lay the fibers onto the springs. The springs were also formed in order to determine if the fibers could be placed onto already existing endovascular devices as a barrier. After the fibers were electro-spun onto the spring, then some of those springs had polyether TPU or aliphatic PC TPU melt blown onto the electro-spun fibers. Figure 4.10 shows the formation of the spring samples. Since the springs were made along with the sheets, it was not determined until after the testing of the sheets which springs would be chosen to undergo testing to determine VSMC migration and platelet activation. After examining all the test results, it was determined that the 10wt% and 15wt% springs would undergo VSMC migration and platelet activation testing.

4.4 Biological Effects

After the tensile, porosity, and fiber diameter tests were performed, the melt blown, electro-spun, and melt blown/electro-spun web sheets and springs were sent to the University of Tennessee Health Science Center at the College of Medicine and the Vascular Biology Center of Excellence in Memphis, Tennessee for in vivo testing. There were three tests performed: (1) vascular smooth muscle cell (VSMC) proliferation in the presence of stimulants, (2) VSMC migration assays, and (3) new platelet activation. After each test was performed the materials were critiqued as to their results in order to determine the best material for an endovascular device [42].

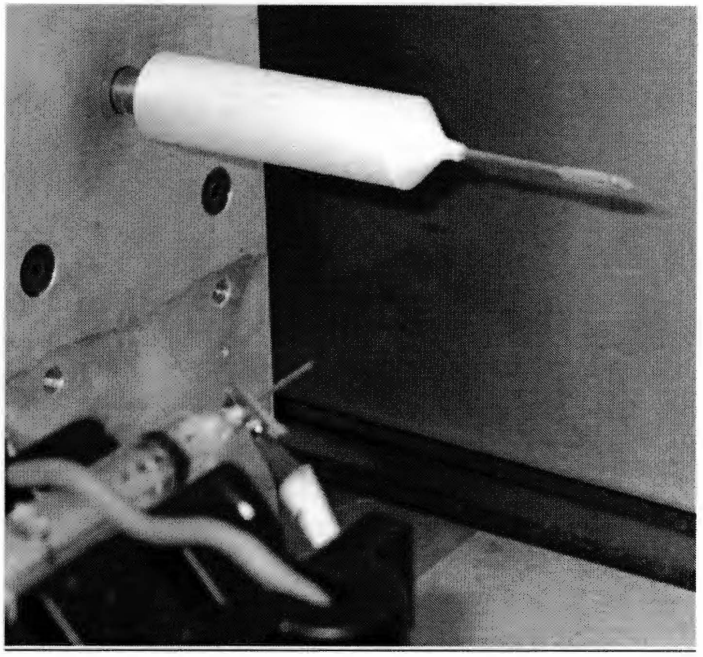

(a)

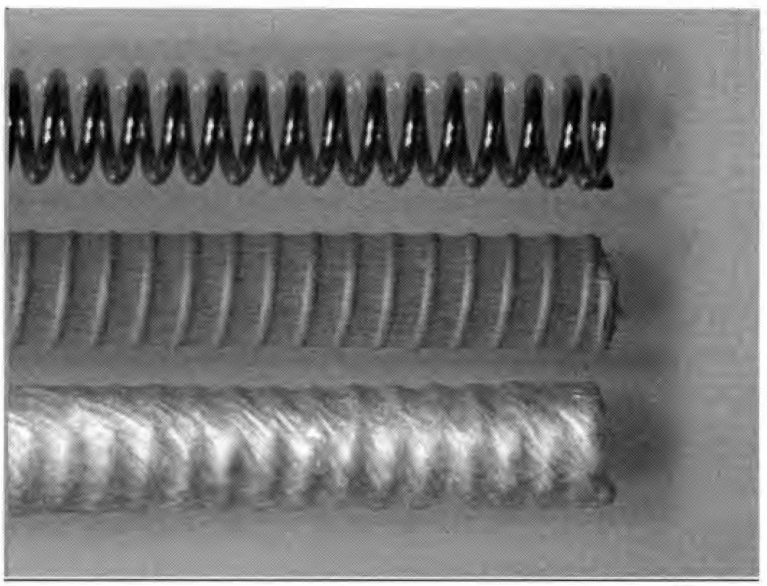

(b)

Figure 4.10: 4mm stainless steel springs: (a) electro-spinning process and (b) top: bare metal spring, middle: electro-spun fiber coated on spring, bottom: melt-blown fibers coated on electro-spun fiber.

A. VSMC Proliferation in the Presence of Stimulants

The VSMC proliferation tests were performed using 5 different fiber coated springs and one non-coated spring. The springs tested were an ES polyether TPU, an ES aliphatic PC TPU, a composite of MB aliphatic PC TPU with ES aliphatic PC TPU, a composite of ES polyester TPU with MB aliphatic PC TPU, a composite of aliphatic PC TPU with polyether TPU, and a bare non-fiber coated spring. Each spring was sterilized for at least 30 minutes with 70% ethanol and dried for at least 6 hours. The ends of the springs were then sealed off with 0.5 cm sterilized strips of Para film on each of its ends. Once the ends were sealed the springs were then placed into 6 well cell culture dishes and equilibrated in the culture media for 12 hours. After 12 hours the media was removed from the spring wells and 8 mL of VSMC suspension was added to each well. There was approximately 200,000 total cells per well. After the first 24 hours the media was changed, then changed again after every 48 hours passed. The proliferation was evaluated at different time intervals until the experiment was complete. Once the experiment was complete the media was removed and the wells were washed with pH 7.4 PBS. The adherent cells were then fixed with 4% Para formaldehyde for 10 minutes. The excess Para formaldehyde was removed and the cells were dyed with 0.1% Crystal Violet for 5 minutes. Figure 4.11 shows the springs within the culture wells before and after they were stained. As can be seen there are shadows being cast by the spring's stimulus, which means that the VSMC are fairly close to the springs. In all, the test showed that there were healthy, proliferating VSMC present [42].

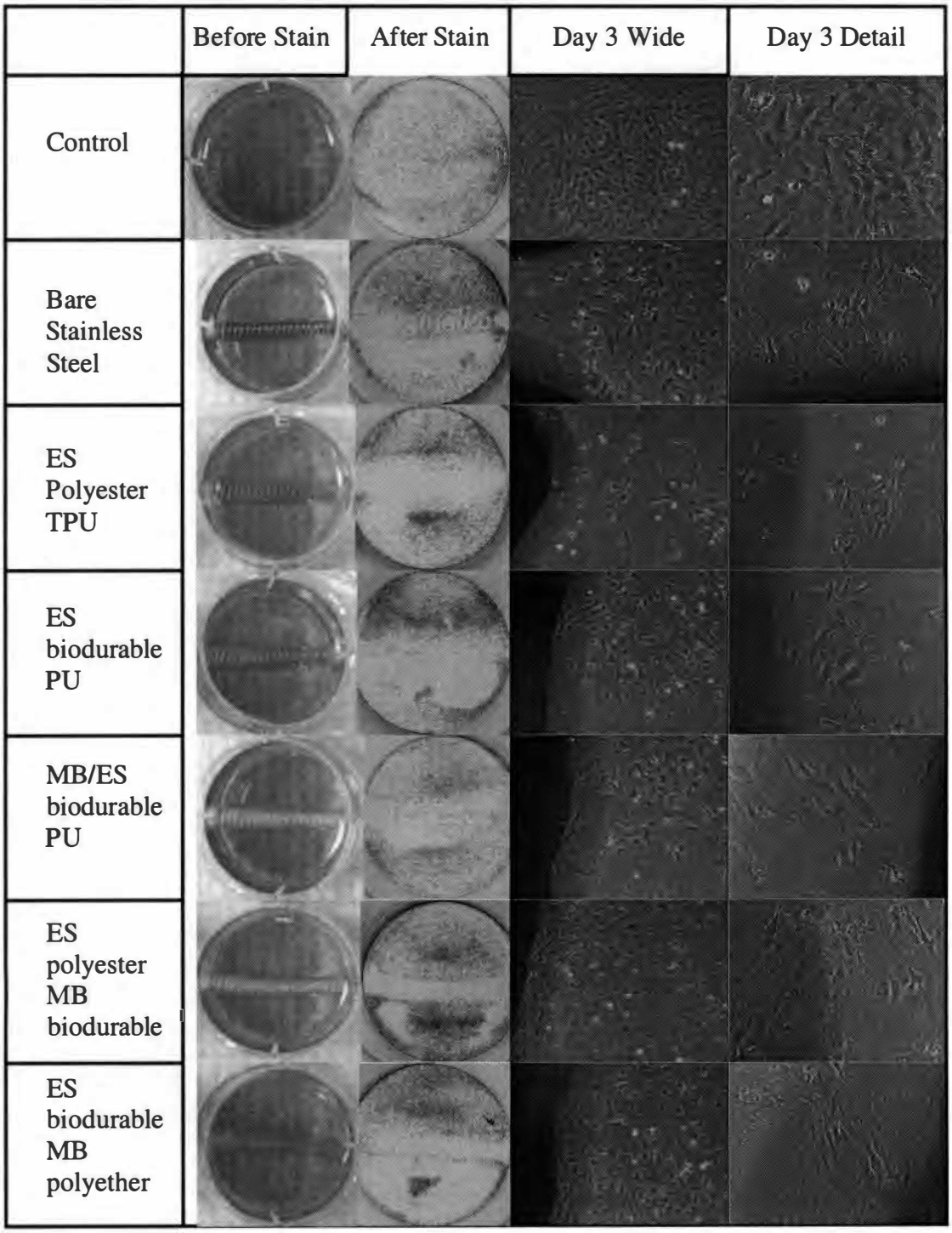

Figure 4.11: Vascular smooth muscle cell proliferation of springs with stimulant results.

B. VSMC Migration Assays

The VSMC migration assay test was performed on some of the web sheets. There were a total of 5 different web sheets tested which were: the MB polyether TPU M1 and M3 web sheet, the ES polyester TPU M1 web sheets, and ES aliphatic PC TPU A1 and A2 web sheets. The test was performed using modified Boyden chambers that consisted of an upper and lower chamber that was separated by a control polycarbonate filter with 8□m pores. The chambers used VSMC's that were harvested at ~70% confluency. The cells were washed twice with a 2.5 x 10^5/mL of culture media. After washing the cells were at rest for 30 minutes at 37 °C in DMEM that was supplemented with 1% (w/v) bovine serum albumin (BSA). After 30 minutes the lower chamber was filled with the cell culture media and 400 □L of suspension was added to the upper chamber for a total of 1 x 10^5 cells/well. The cells were left to migrate for 18 hours at 37 °C with 5% CO_2. After 18 hours the upper chamber was aspirated and washed with pH 7.4 PBS and both chambers were disassembled in order to remove the membranes. Next, the upper surface of each membrane was gently scraped in order to remove the cells that had adhered to the membranes. The membranes were then washed with PBS and fixed with 4% Para formaldehyde for 10 minutes. The excess Para formaldehyde was removed so that the membranes could by dyed with 0.1% Crystal Violet for 5 minutes. Lastly, the contents in the lower chamber were placed into a tube and spun at 136 xg for 5 minutes. The cell pellets that resulted from the spinning were then suspended in 25 □L PBS and counted by a hermacytometer.

In the end, figure 4.12 shows the results of the test. As can be seen the ES materials had the lowest percentage of cell migration. The polyester TPU M1 sample had

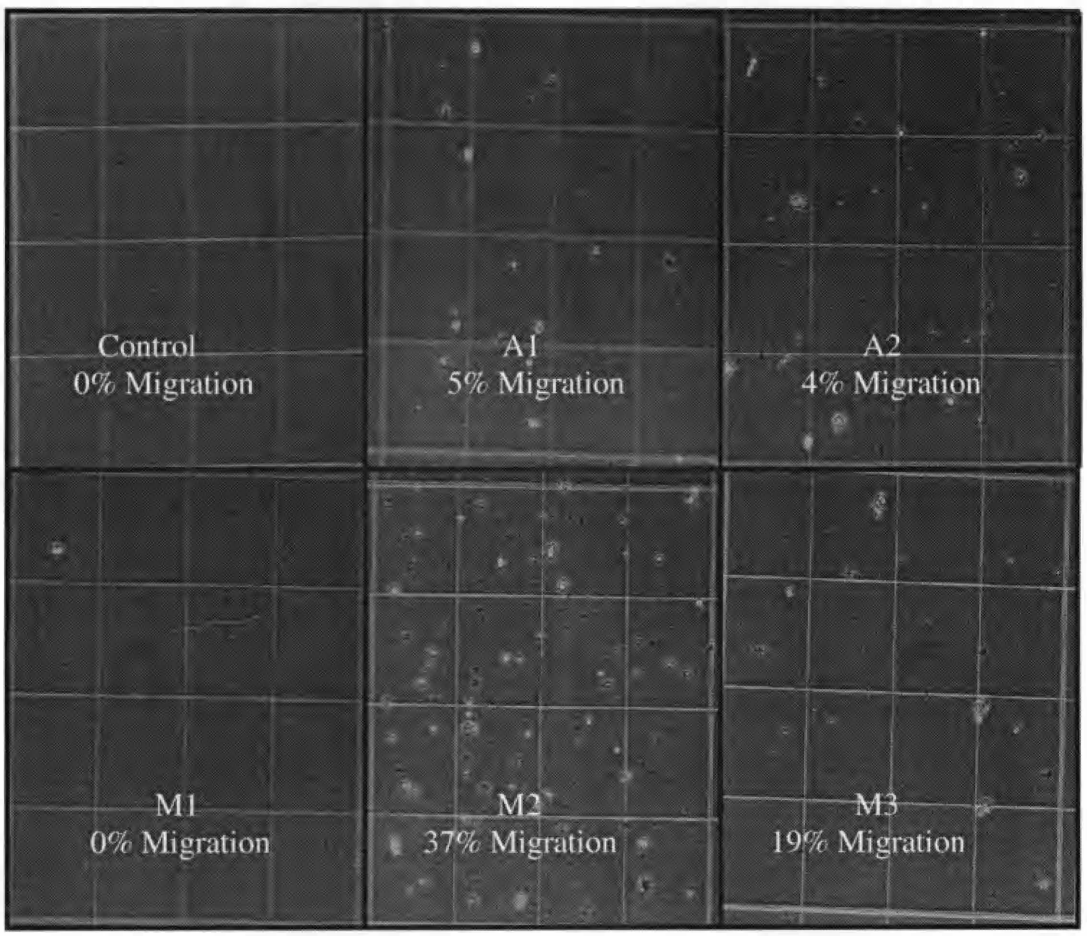

Figure 4.12: Vascular smooth muscle cell migration assay results.

0% cell migration and the electro-spun aliphatic PC TPU A1 and A2 samples showed 4-5% cell migration. On the other hand, the MB materials had high cell migration. The MB polyether TPU M1 sample had 19% cell migration while the polyether TPU M3 had a 38% cell migration. Overall, the cell migration results indicate what the porosity results showed, which was that the MB samples have larger pores. The large pores allow cells to migrate through the sample easier than if the pores were small. The smaller the pores, the better the material is at deterring cell migration, which is the objective of this research [42].

C. Platelet Activation

The last test performed was the platelet activation test that was performed using the composite of MB and ES web sheets of 10wt% and 15wt%. The sheets used were from the composite of MB polyether TPU with ES polyester TPU and the composite of MB aliphatic PC TPU with ES aliphatic PC TPU (MEP1, MEP2, MEP3, MEA1, and MEA2). Each sample was sterilized then cut into 1.3 cm diameter discs, which were then placed into some of the wells of a 24 well cell culture plate. The wells that did not contain a sample were used as negative controls. All the wells had 500 ▯l aliquot of PRP added to themselves. Next, ADP at a 20.▯M concentration was added to some of the wells in order to provide both a positive control and an activating stimulus that could possibly promote adhesion. After the ADP was added, the plates were manually swirled for several seconds in order to ensure the ADP was mixed. Next, the plates put at rest for one hour at 30°C. After one hour the plates were gently swirled again. Then the aliquots were removed from the wells and underwent cytometric analysis.

The cytometric analysis was performed in order to examine the expression of the platelet membrane glycoprotein CD62. 50 ▯L of the platelet suspensions were incubated with 15 ▯L of antibody for 15 minutes at 37 °C. After 15 minutes the sample was analyzed by a FACSCalibur station for bound chromophore. For control for a nonspecific antibody binding, a murine IgG was used. A mean fluorescent intensity (MFI) was used as a surface expression marker. If the MFI was intense that meant they were bound to the chromophore. The more intense the MFI, the more bound chromophore there are. The more bound chromophore there is, the higher the surface expression of the activation marker, which means more platelet activation. For the samples tested there was no significant platelet activation except with the positive control. However, the positive control was meant to increase. In all, the MFI's for the ADP- sample wells were about the same as the ADP-IgG control and ADP-CD62 [42].

V. Conclusions

In this study, samples of different polyurethanes were formed into nonwoven webs through melt blowing and electro-spinning processes. The nonwoven webs were tensile strength, porosity, and fiber diameter tested. Some of the web coated springs and sheets were in vivo tested in order to determine if the webs were formed so that they would impair VSMC migration and activate platelets. Comparisons were made of the mechanical properties and biological properties for each web material tested. Based on the results obtained from the research, the following conclusions were made.

a. Comparison of the average pore diameters of the all the web sheets revealed that there were three web sheets that had pore diameters small enough to impair VSMC migration. The composite of MB polyether TPU with 15wt% ES polyester TPU, the composite of MB aliphatic PC TPU with 10wt% ES aliphatic PC TPU, and the 15wt% ES polyester TPU web sheets had the lowest pore diameters.

b. Comparison of the average forces handled by all the web sheets revealed that the composite of MB polyether TPU with 10wt% ES polyester TPU and the composite of MB aliphatic PC TPU with 15 wt% ES aliphatic PC TPU were overall the stronger web materials over the other web sheets. A tensile strength test on the MB web sheets and the composite MB and ES web sheets supported the findings.

c. Comparison of the fiber diameters of all the webs tested revealed that the aliphatic PC TPU webs had smaller fiber diameters whether

they were ES or a composite of MB and ES. An examination of the SEM photographs of all the tested webs supported the finding by showing that the other webs had much larger fiber diameters.

d. Examination of in vivo tests revealed that ES and the composite of MB and ES web sheets and web coated springs were better suited for VSMC proliferation and migration and for platelet activation. The VSMC proliferation and migration and the platelet activation test results support the finding.

e. Comparing and analyzing the tensile strength, porosity, fiber diameter, and in vivo tests revealed that the composite MB polyether TPU and 15wt% ES polyester TPU webs were the overall better material to inhibit VSCM migration and for new platelet activation.

VI. Recommendations

Based on the results presented in the thesis, future research should include:

1. The technique to control the thicknesses and weights of the melt blowing and electro-spinning processes in order to form more uniform nonwoven fibers.
2. The use of drug elution in the materials in order to provide better blockage of VSMC proliferation and migration, and to activate new platelets.
3. In vitro tests in the appropriate animal specimens to ensure that the device was acceptable for implantation.

LIST OF REFERENCES

List of References

1. Li, D. and Xia, Y. (2004). *Electrospinning of Nanofibers: Reinventing the Wheel.* Advanced Materials, 16, 1151-1170.
2. Vascular Grafts (n.d.) Retrieved on November 16, 2006. www.surgical-tutor.org.
3. Malkan, Sanjiiv R and Wadsorth, Larry C. (1991). *A Review on Melt Blowing Technology.* INB Nonwovnes, p.1.
4. Horrocks, A.R. and Anand, S.C. *Handbook of Technical Textiles.* Woodhead Publishing (2002).
5. McAmish, L.H., Addy, T.O., and Lee, G.F. (1986). *Nonwoven Medical Fabric.* U.S. Patent 4,622,259.
6. Pinchuk, L.S., Goldade V.A., Makerevich, V.A., and Kestleman, V.N. (2002). *Melt Blowing Equipment, Technology, and Polymer Fibrous Materials.* New York: Springer-Verlog Berlin Heidelberg.
7. *Thermoplastic Materials.* Retrieved October 3, 2006. www.globalspec.com
8. DeWitt Company-Landscape and Plant Fabrics (n.d.) Retrieved on September 3, 2006. www.dewittcompany.com
9. Ratner, Buddy D., Hoffman, Allan S., Schoen, Frederick J., and Lemons, Jack E. *Biomaterials Science.* 2nd Ed. Elsevier Academic Press. Boston, Massachusetts (2004).
10. Grafe, Timothy H. and Graham, Kristine M. (2003). *Nanofiber Webs from Electrospinning: Nonwovens* .Minneapolis, Minnasota: Donaldson Company Inc.

11. Deitzel, J.M., Kleinmeyer, J., Harris, D., and Beck Tan, N.C. *The effect of processing variables on the morphology of electrospun nanofibers and textiles.* Polymer, 42 (2001), p.261-272.

12. Electrostatic Spinning of Nanofibers Spin Technologies, Chattanooga, Tennessee.

13. Fong, H., Chun, I., and Reneker, D.H. *Beaded nanofibers formed during electrospinning*. Polymer, 40 (1999), p. 4585-4592.

14. Zong, Xinhua, Kim, Kwangsok, Fang, Dufei, Ran, Shaofen, Hsaio, Benjamin S., and Chu, Benjamin. *Structure and process relationship of electrospun bioabsorbable nanofiber membranes.* Polymer, 43 (2002), p. 4303-4412.

15. Buchko, C.J., Chen, L.C., Yu, Shen, and Martin, David C. *Processing and microstructural characterization of porous biocompatible protein polymer thin films*. Polymer, 40 (1999), p. 7397-7407.

16. Polyurethane (n.d.) American Chemistry Council, Inc. Arlington, VA (2006). www.polyurethane.org/about/history.asp

17. Oertel, G. (1993). Polyurethane Handbook. (2nd ed.). New York: Hanser Gardner Publications.

18. Szycher, M. (1999). *Szycher's Handbook of Polyurethanes*. CRC Press LLC. New York, N.Y.

19. Xiao, H. and Frisch, K. (1995). *Advances in Urethane Ionomers.* Pennsylvania: Technomic Publishing Company, Inc.

20. Lee, Youn E. (August 2004). *Process Property Studies of Melt Blown Thermoplastic Polyurethane Polymers*. Dissertation. University of Tennessee, Knoxville.

21. Gale, Thomson. (2006). *Polyurethane*, Thomson Corp., v6. www.madehow.com/Volume-6/Polyurethane.html

22. Correspondence with Lenhart, D. Nonwovens, Inc. (2005).

23. Hasirci, Nesrin and Hasirci, Vasif. (2003). *Biomaterials: from molecules to engineered tissues.* New York: Kluwer Academic/ Plenum Publishers.

24. Ratner, Buddy D., Hoffman, Schoen, Allan S. , Frederick J. and Lemons; Jack E., (2004) *Biomaterials Science: An Introduction to Materials in Medicine.* New York: Elsevier Academic Press.

25. Noveon, Inc. (n.d.) Retrieved on March 2006. www.noveon.com

26. Correspondence with Dr. Roberto Benson (2006).

27. Stevens, Malcolm P. *Polymer Chemistry: An Introduction.* Oxford University Press, Inc. New York (1999).

28. Gibson, Phillip, Gibson, Heidi Screuder, and Rivin, Donald. *Transport properties of porous membranes based on electrospun nanofibers, Colloids and surfaces A: Physicochemical and Engineering Aspects.* 187-188 (2001), p. 469-481.

29. SEM (n.d.). Retrieved September 16, 2006 from www.mos.org.

30. Goldstein, Joseph I., Romig Jr, A.D., Dale, E., Lyman, Charles E., Echlin, Patrick, Fiori, Charles, Joy, David C., and Lifshin, Eric. *Scanning Electron Microscopy and X-ray microanalysis,* 2nd Ed. (1992).

31. Wadsworth, L.C. and S.R. Malkan. *A Review of Melt Blowing Technology.* INB, Nonwovens, p2 (1991).

32. Dahiya, Atul, M.G. Kamath, and Raghavendra R. Hedge. Melt Blowing Technology. The University of Tennessee, Knoxville (April 2004). www.engr.utk.edu/mse/pages/Textile.html

33. Becton, Dickinson and Company. (2006) www.bd.com

34. Capillary Flow Porometer (n.d.) Retrieved October 5, 2006. www.pmeapp.com

35. United Calibration. (n.d.). Retrieved on October 6, 2006. www.tensiletest.com

36. Image Pro Plus (n.d.). Retrieved October 5, 2006 form www.scitech.com

37. Aliphatic PC Thermoplastic Polyurethane (n.d.). Retrieved on May 30, 2006 from Noveon, Inc..

38. Estane 54245 TPU (n.d.). Retrieved on October 13, 2005 form www.estane.com

39. Estane 58238 TPU. (n.d.) Retrieved on May 30, 2006 from www.estane.com

40. Zapletalova, Terezie, Micheilsen, Steven, and Pourdeyhimi, Behnam. *Polyether Based Thermoplastic Polyurethane Melt Blown Nonwovens*. Journal of Engineered Fabrics. v.1 issue 1 (2006).

41. TPU Processing Information. The Plastics Web. (n.d.) Retrieved on May 2006. www.ides.com

42. Personal Correspondence with Henry Speich. the University of Tennessee Health Science Center at the College of Medicine and the Vascular Biology Center of Excellence in Memphis, Tennessee, 2006.

Vita

Constance R. Eastman was born in Washington State on February 23, 1979. She attended several schools across the nation before graduating from high school at Ooltewah High School in Ooltewah, Tennessee in 1997. She received a Bachelor of Science degree in Mechanical Engineering from the University of Tennessee, Knoxville. During her undergraduate years, she worked for the University of Tennessee, Knoxville and for the Tennessee Valley Authority in Spring City, Tennessee. She continued her higher education at the University of Tennessee, Knoxville, where she will receive her Master of Science degree in Polymer Engineering with a concentration in Textiles in December.

5873 8321 13
04/04/07 VG THGroup